Corrosion of steel in concrete at various moisture and chloride levels

Johan Ahlström

LUNDS
UNIVERSITET

Licentiate Thesis, Report TVBM-3178, Division of Building Materials,
Faculty of Engineering, Lund University, Lund 2014

Lund University
Division of Building Materials
www.byggnadsmaterial.lth.se

ISRN LUTVDG/TVBM--14/3178--SE(1-31)
ISSN 0348-7911 TVBM

Printed in Sweden by Media-Tryck, Lund University
Lund 2014

Preface

The work presented in this licentiate thesis has been carried out partly at the Division of Building Materials, Lund University, and partly at Swerea KIMAB, Stockholm. The work was started in June 2011 and has been funded by Elforsk AB (Swedish Electrical Utilities R&D Company), SBUF (The development Fund of the Swedish Construction Industry) and Swerea KIMAB, to whom I am very grateful.

I would like to thank my supervisors Professor Lars Wadsö (Lund University), Johan Tidblad (Swerea KIMAB) and my associate supervisor Adjunct Professor Manouchehr Hassanzadeh for providing me with their expertise and experience. I would also like to thank my colleges Bertil Sandberg and Bror Sederholm for their valuable contributions to this work.

Finally, I would finally like to thank my employer Swerea KIMAB for encouraging postgraduate studies while working at the institute.

Stockholm, July 2014
Johan Ahlström

Summary

About 7000 concrete bridges in Sweden were built before 1965. The annual cost for maintenance of these bridges is about 0.6% of their total value. The cooling water tunnels at Swedish nuclear power plants have been exposed to seawater for about 30-40 years. The maintenance cost for these tunnels has been evaluated to be about one billion Swedish kronor. It is important to evaluate the risk of corrosion for these types of structures and due to the relatively their old age, corrosion of steel in concrete might be an increasing problem in the future.

Generally, corrosion of steel in concrete is induced by either carbonation or by chlorides. Carbonation means that carbon dioxide in air reacts with calcium within the concrete. This means that the pH of the concrete is decreasing and the steel start to corrode. Chloride induced corrosion means that chlorides are transported through the concrete to the steel and the corrosion rate can then increase significantly. It has been proposed in the literature that a certain chloride threshold level exist where an initiation of a significantly high corrosion rate occur. For decades, researchers have been trying to determine this chloride threshold level and the results scatter to a large extent. This is probably due to many different experimental setups and different properties of the used steel and concrete. One important factor to consider is the moisture condition of the concrete. It is generally accepted that the corrosion rate of the steel is low in dry concrete due to high resistivity. For very wet concrete, the corrosion rate is also low due to slow transportation rate of oxygen to the steel surface. At an intermediate moisture condition, the corrosion rate is high due to relatively low resistivity and high transportation rate of oxygen.

In the present study, samples made of steel cast in chloride containing mortar were exposed to different moisture conditions. The moisture condition was either static at a certain relative humidity or dynamic where the relative humidity was cycling between 75% and 100%. The lowest chloride concentration which caused initiation of corrosion was 1% Cl by mass of cement and was measured for samples exposed to 97% RH. At higher or lower moisture conditions than 97% RH, the corrosion rate was lower. For samples exposed to dynamic moisture conditions, the lowest chloride concentration which initiates corrosion was measured to be 0.6% Cl by mass of cement. Based on these results it was suggested that the chloride threshold

level is lower than 1% Cl by mass of cement for samples exposed to static moisture conditions and even lower chloride concentration can initiate corrosion in dynamic moisture conditions.

The present study also assessed the corrosion properties of steel in a cooling water tunnel. The corrosion potential was measured during one year and it was found that the steel in concrete was in an electrical connection with water pumps made of stainless steel and in contact with sacrificial anodes. The connection with the pumps increased the corrosion potential and the connection with the sacrificial anodes decreased the corrosion potential. To assess if there is an increased risk of galvanic corrosion due to the connection with the pumps, a complementary study was made to measure potentials where the corrosion increase significantly. The results suggested that it is not likely that the steel in the tunnel suffer of galvanic corrosion, due to that the measured corrosion potentials in the tunnel was lower than the measured potentials in the complementary study.

Keywords: Steel, rebar, concrete, corrosion, chloride threshold level, moisture.

Sammanfattning

Ungefär 7000 betongbroar i sverige byggdes före 1965. De årliga underhållskostnaderna för dessa broar motsvarar ungefär 0.6% av deras totala värde. Kylvattenvägar i svenska kärnkraftverk har varit exponerade mot saltvatten i ungefär 30-40år. Reparationskostnader för dessa kylvattenkonstruktioner har uppskattats till ungefär en miljard kronor. På grund av den relativt höga åldern på dessa betongkonstruktioner kan korrosion bli ett växande problem i framtiden.

Vanligen så initieras korrosion på stål i betong antingen av karbonatisering eller av klorider. Karbonatisering betyder att koldioxid reagerar med kalcium som finns i betongen. Detta orsakar att pH nivån sänks i betongen och stål börjar därför korrodera. Kloridinducerad korrosion betyder att klorider transporteras genom betongen fram till stålet och stålets korrosionshastighet kan då öka kraftigt. I litteraturen har det diskuterats att det finns ett kloridtröskelvärde som måste uppnås för att initiering av en signifikant hög korrosionshastighet skall kunna inträffa. Det har gjorts många försök för att fastställa detta kloridtröskelvärde men resultaten varierar mycket. Detta beror troligen på att det finns många olika typer av försökuppställningar och egenskaper på stål och betong som har använts i försöken. En viktig faktor att ta hänsyn till är betongens fukttillstånd. Det är generellt sett accepterat att korrosionshastigheten för stål i torr betong är låg på grund av hög resistivitet. I väldigt fuktig betong är också korrosionshastigheten låg på grund av långsam transport av syre. I ett mellanhögt fukttillstånd kan korrosionshastigheten vara hög på grund av relativt låg resistivitet och relativt hög transporthastigen för syre.

I denna studie har prover tillverkats av stål ingjuten i bruk innehållande klorider. Proverna har sedan exponerats i ett statiskt fukttillstånd vid en specifik relativ fuktighet eller i ett dynamiskt fukttillstånd där den relativa fuktigheten växlade mellan 75% och 100%. Den lägsta kloridkoncentrationen som initierade korrosion uppmättes vara 1% Cl per cementvikt för prover som exponerades i 97% relativ fuktighet. Vid högre eller lägre fuktighet än 97% så uppmättes korrosionshastigheten vara lägre. För prover som exponerats i dynamiska fukttillstånd uppmättes den lägsta kloridkoncentrationen till 0.6% Cl per cementvikt. Baserat på dessa resultat så har det föreslagits att kloridtröskelvärdet är lägre än 1% Cl per cementvikt vid statiska fukttillstånd och ännu lägre vid dynamsika fukttillstånd.

I denna studie så utvärderades också stålS korrosionsegenskaper i betong vid en kylvattentunnel. Korrosionspotentialen uppmättes under ca ett år och det kunde konstateras att stålet i betong var i en elektrisk kontakt med vattenpumpar gjorda av rostfritt stål samt i kontakt med offeranoder. Kontakten med pumparna orsakade högre korrosionspotentialer och kontakten med anoder orsakade lägre korrosionspotentialer. För att utvärdera om det fanns en risk för galvanisk korrosion orsakad av pumparna gjordes en komplementerande studie för att mäta potentialer där korrosionshastigheten kraftigt ökar. Av resultaten så framgick det att det troligen inte finns en förhöjd risk för galvanisk korrosion eftersom de uppmätta potentialerna i tunneln var lägre än de uppmätta potentialerna i den komplementerande studien.

Nyckelord: Stål, armering, betong, korrosion, kloridtröskelvärde, fukt.

List of Publications

PAPER I **Galvanic corrosion properties of steel in water-saturated concrete**
Ahlström, J. Tidblad, J. Sandberg, B. Wadsö, L.
Published (early view) in ”Materials and Corrosion”. 2013, XXX, No. XXX

PAPER II **Influence of chloride and moisture content on steel rebar corrosion in concrete**
Ahlström, J. Tidblad, J. Wadsö, L
Submitted.

Contents

1 Introduction

1.1 Background

Deterioration of concrete structures may have several explanations e.g. alkali-silica reaction, frost damage, acid attack and sulphate attack. However, the most frequent deterioration mechanism is arguably corrosion of reinforcement steel in concrete. Corrosion of steel in concrete is induced either by carbonation or by chlorides. As it takes time before the carbonation front or the chloride ions reach the steel, there is a period before corrosion is initiated cf. Tuutti 1982. The duration of this period is dependent on the concrete quality, the thickness of the concrete cover and environmental parameters. In chloride-containing environments such as marine environments or where road salt is used, the corrosion rate of steel in concrete can increase significantly, once the corrosion has started. One very important factor for corrosion and almost all other concrete deterioration mechanisms is the moisture condition of the concrete. For concrete with low moisture content, the corrosion rate is low due to high resistivity, and for concrete with very high moisture content, the corrosion rate is low due to slow transport of oxygen. For intermediate moisture content, the corrosion rate can be high due to relatively low resistivity and high transport of oxygen.

It is important to evaluate the risk of corrosion of steel in concrete structures. One example of where this is important is the approx. 7000 road bridges in Sweden that were built before 1965 Manouchehr Hassanzadeh (2014). The annual cost for maintenance of these bridges is about 0.6% of the total value of the bridges and rebar corrosion is an important aspect to consider. Another example is the cooling water tunnels at Swedish nuclear power plants that have been exposed to seawater for about 30-40 years and the maintenance cost of these tunnels have been evaluated to be about one billion Swedish kronor. This could mean that problems with rebar corrosion might increase in the future.

1.2 Objective

The objectives were to

- Perform a laboratory study to assess corrosion of steel in mortar at various moisture and chloride levels.
- Determine corrosion potentials where the risk of corrosion for steel in water-saturated concrete increases.
- Investigate the corrosion properties in a cooling water tunnel.

1.3 Limitations

This thesis investigates the corrosion of steel in mortar exposed to different chloride and moisture levels. Other types of deterioration mechanisms are not included.

2 Corrosion of steel in concrete

2.1 Corrosion properties of steel in concrete

Corrosion can be described by electrochemical reactions where the anodic (electron-producing) reaction, is e.g. oxidation of iron. The cathodic (electron-consuming) reaction is determined by the properties of the electrolyte. For corrosion in concrete, the cathodic reaction is oxygen reduction. The mentioned reactions for corrosion of steel in concrete are:

$2Fe \rightarrow 2Fe^{2+} + 4e^-$	anodic reaction, oxidation of iron
$O_2 + 2H_2O + 4e^- \rightarrow 4OH^-$	cathodic reaction, oxygen reduction

The reactions occur simultaneously at different areas on the steel surface, called anodic and cathodic areas. The corrosion system is defined as a steel surface exposed in concrete where an electrochemical cell is formed. An electrochemical cell is composed of an anodic and cathodic area, an electron conductor, which is the rebar and an ion conductor, which is an electrolyte. The pore water in concrete functions as an electrolyte.

Steel in concrete is naturally in a passive state, which means that the corrosion rate is low due to the high pH of the pore water solution. The steel surface in the passive state has a protective layer where the composition of the layer is determined by pH and the potential. The passive layer can have different chemical compositions with different amounts of hydroxides/oxides/oxyhydroxides. In chloride contaminated concrete, the passivity can be broken which means that the passive layer is not protective. This means that the steel surface is in an active state where the corrosion rate increases. The following discussion of rebar corrosion is for corrosion where the concrete is contaminated by chlorides.

The corrosion rate of steel in concrete is determined by the properties of the steel, the properties of the concrete and the properties of the environment. The properties

of steel may include the chemical composition and surface characteristics such as with/without a mill scale. The properties of concrete may include the water/cement-ratio and type of cement. These properties are discussed more in detail under section 2.4. Figure 1 shows four different environments which affect the corrosion rate of steel in concrete. The first environment marked as 1 illustrates steel in concrete placed at a waterline. The concrete will have different moisture conditions from dry concrete in air to wet concrete in water. The moisture condition is discussed in more detail in section 2.2.2. The second environment marked as 2 is steel in water-saturated concrete connected to a more noble material than carbon steel, and this type of environment is discussed in more detail in section 2.2.3. The third environment is steel in concrete which is connected to a material which is less noble than carbon steel, this type of environment is discussed in more detail in section 2.2.4. The fourth type of environment is steel in carbonated concrete.

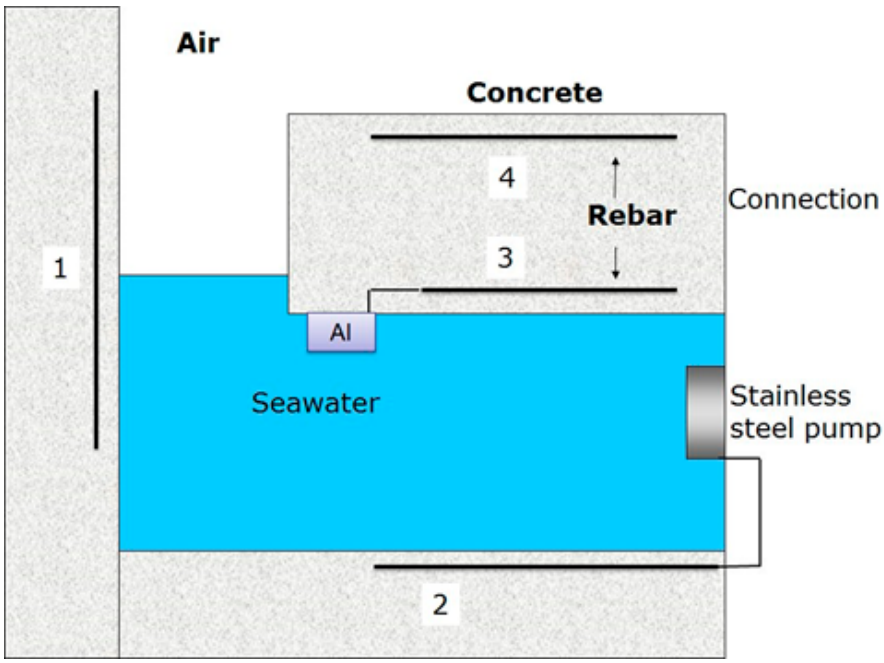

Figure 1. A schematic figure of a concrete structure where a rebar is: 1) exposed to concrete with different moisture conditions. 2) connected to a more noble material. 3) connected to a less noble material. 4) exposed to carbonated concrete.

2.1.1 Chloride threshold level

Corrosion of steel in concrete was described by Tuutti (1982) as two distinct time steps, see Figure 2. The first step is where chlorides are transported through the

concrete cover to the steel surface causing initiation of corrosion. Initiation occurs when the chloride concentration at the steel surface has reached the chloride threshold level. The last step is the corrosion propagation. The chloride concentration that is needed to initiate corrosion is usually called the chloride threshold level (CTL).

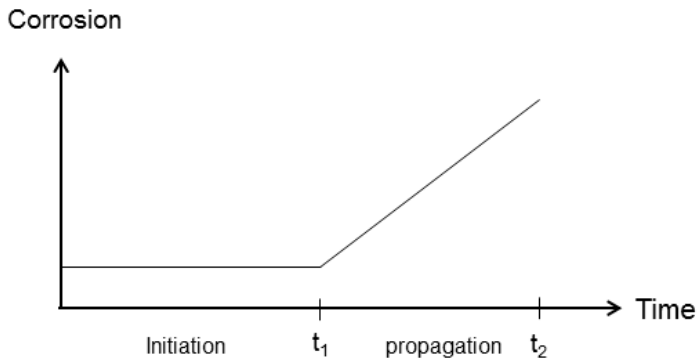

Figure 2. Corrosion model of corrosion of steel in concrete suggested by Tuutti.

Chloride is either bound in the concrete material or free in the pore water. Therefore, CTL can be expressed in different ways. An early study by Hausmann (1967) suggested that that CTL may be expressed as the ratio of the hydroxide concentration and the chloride concentration in the concrete pore water. This ratio was measured to be 0.6. A later study by Glass & Buenfeld (1997) suggested that CTL can be expressed as the total concentration of chlorides by mass of cement. Hereafter the term % Cl by mass of cement will simply be expressed as % Cl. This includes the free chlorides in the pore water and the bound chlorides. Alonso et al. 2002 measured the CTL to be 0.4% Cl with an electrochemical method.

For reported studies in natural conditions, the CTL has been measured from close to 0 to 2.5% Cl according to Melchers & Li (2009). Several studies have been conducted to measure CTL and the value differs several decades both from laboratory studies and field studies which is shown in a state of the art report by Angst et al. (2009). Sandberg (1999) performed a field study at the Swedish west coastline and reported CTL values between 0.6 and 1.2% Cl.

The large scatter of reported CTL reveals that it is difficult to measure CTL. It was reported by Silva (2013) that chlorides are accumulated at anodic sites on the steel surface even prior to activation of the steel. Therefore, the chloride concentration at anodic sites may be higher than the chloride concentration in the bulk pore water solution. Moreover, the concentration of chlorides in the pore water may naturally differ in different areas of the concrete, even at the same cover depth. This was

shown in a study performed by Angst et al. (2011). This may in part explain the difficulty of measuring CTL.

The chloride threshold level has been reported to be lower for steel with the mill scale intact compared to steel with removed mill scale. It was suggested by Ghods et al. (2010) that hidden crevices between the steel surface and the mill scale are susceptible sites for pitting corrosion. This may explain why lower CTL is reported for steel with mill scale.

2.1.2 Moisture dependency for corrosion

The relative humidity (RH) of air is described as:

$$RH = \frac{v}{v_0} \qquad (1)$$

where, v is the water vapour content, v_0 is the saturated water vapour content at a certain temperature.

A pore system is formed in concrete with a certain pore size distribution. Small pores are more easily filled with capillary condensed water compared with large pores according to the Kelvin equation:

$$\ln(RH) = \frac{2\gamma V_m}{rRT} \qquad (2)$$

where γ is the surface tension of water, V_m is the molar volume of water, r is the pore radius, R is the standard gas constant and T is the temperature. This means that different types of concrete with different pore systems will have different amount of capillary condensed water. The amount of capillary condensed water (previously called pore water) is important as this water will act as an electrolyte on the steel surface and affect the resistivity of the concrete.

Corrosion of steel in concrete is dependent of the moisture condition in the concrete. This is due to that moisture affects both the resistivity of the concrete and the diffusion rate of oxygen. The resistivity is high in dry concrete, which means that the corrosion rate is slow and that the corrosion rate is under ohmic control. The resistivity in water-saturated concrete is low but on the other hand, the diffusion rate of oxygen is slow compared to the diffusion rate in dry concrete. This means that the corrosion rate is slow and that the corrosion rate is under diffusion control. Tuutti (1982) reported that the corrosion rate reaches a maximum at a certain moisture condition where the resistivity is relatively low and the oxygen transportation rate is relatively high.

A study performed by Pettersson (1997) exposed steel in mortar at different moisture levels. The CTL was measured with an electrochemical method; the linear polarisation resistance method (LPR). The results showed that the lowest CTL

was 0.5% Cl at 90% RH. It should be noted that it may be difficult to measure corrosion rates of steel in concrete with different moisture conditions with LPR. This was suggested by Millard et al. (2001).

Michel et al. (2013) showed that when steel in concrete is in a passive state, the corrosion rate is not affected by the moisture condition of the concrete. When steel is corroding, in an active state, the corrosion rate is affected by the moisture condition. Three different critical pore saturation levels were suggested by Lopez & Gonzalez (1993), one called an upper critical pore saturation limit, PS_{uc}, which is the pore saturation where the maximum corrosion rate is obtained (pore saturation is the fraction of the pore space that is filled). The PS_{uc} was suggested to be 70% and correspond to the resistivity $7x10^3$ Ωcm. The second was called lower critical pore saturation, PS_{lc}, and was suggested to be 35% and corresponds to the pore saturation where corrosion stops. The third was called practical pore saturation at PS_{pc}, and was suggested to be about 45%. This critical saturation corresponds to where the corrosion current density is about 0.1μA/cm^2 and a corresponding resistivity of 10^5 Ωcm. It should be noted that full saturation was defined as when the sample had been in boiling water for two hours; this should not be confused with capillary water saturation, which occurs in atmospheres when the RH is below 100%.

The moisture condition in the concrete affects the resistivity of the concrete and subsequently corrosion. In a literature review performed by Hornbostel et al. (2013) it was stated that there is an overall inverse relationship between resistivity and corrosion, but that there is a scatter between studies.

2.1.3 Rebar connected to a noble material

Carbon steel in concrete may unintentionally be in contact with a more noble material. As an example, if steel in chloride-contaminated concrete is in contact with stainless steel, which is not cast in concrete, the corrosion rate of the rebar increases. This is due to that the formed mixed potential between stainless steel and carbon steel is more anodic than the corrosion potential of carbon steel by itself.

The difference in corrosion potential between stainless steel cast in concrete and carbon steel cast in concrete is relatively small. This means that the corrosion rate of carbon steel is not significantly raised. In chloride contaminated concrete the difference in corrosion potential can be high but the corrosion rate of carbon steel is still determined by the diffusion rate of oxygen. Abreu et al. (2002) showed in a study that there is not a significant risk of galvanic corrosion when carbon steel and stainless steel are electrically connected and cast in young uncontaminated concrete.

Steel in concrete is either in a passive state with a negligible corrosion rate or in an active state with a corrosion rate that is not negligible. Rebars are in passive state in uncontaminated concrete and active state in e.g. carbonated concrete. Nasser et al. (2010) showed that the corrosion rate of steel in carbonated concrete increased when there was an electrical contact with steel in sound concrete.

2.1.4 Rebar connected to a less noble material

To protect or decrease the corrosion rate of steel in concrete, a less noble material can be mounted on the concrete surface that is electrically connected to the rebar. This is called a sacrificial anode. When a sacrificial anode is used, a mixed potential is formed between the sacrificial anode and rebar which is lower than the corrosion potential of the rebar. This means that the rebar is polarized in a cathodic direction to a low potential where the corrosion rate is low or negligible. An example of a sacrificial anode material is aluminium that can be mounted on concrete surfaces in seawater to prevent rebar corrosion. Most of the protection will occur under the seawater level, but there may also be some protection of the concrete above the waterline as long as the resistivity is not too high. Parthiban et al. (2008) used a sacrificial anode made of magnesium with a technical service life of three years. The magnesium anode was cathodically protective initially but the potential of the rebar increased slowly during time. The slow increase was attributed to that chlorides were transported away from the steel surface and the steel obtained more noble potentials.

Another example of a sacrificial anode is zinc that is added on the concrete surface by thermal spraying. The formed zinc layer is connected to the rebar and will protect the rebar beneath the layer, this was tested by Sederholm & Selander (2011). The protection from the zinc layer is self-regulating, meaning that when the concrete is wet, both the current demand and the cathodic protection will be high. When the concrete is dry the corrosion rate of the rebar will be low and the cathodic protection low due to high resistivity. Generally, zinc dissolves in solutions with high pH meaning that the adhesion of the layer onto the concrete surface may be poor if corrosion products are formed on young concrete with high pH. The thickness of the zinc layer is generally from 300 to 400 μm, and if the concrete is exposed in seawater, the consumption rate will be high and protective during a relatively short time period. If the concrete surface is carbonated and has a low pH value, the adhesion between the zinc layer and concrete surface will be better.

2.1.5 Carbonation of concrete

When concrete is exposed to air, the outermost surface is carbonated. This means that calcium hydroxide in the pore water reacts with carbon dioxide in air according to:

$$Ca(OH)_2 + CO_2 \rightarrow CaCO_3 + H_2O$$

An effect of carbonation is that the pH of the pore water is lowered to a level where carbon steel is not passive. The rate of carbonation is controlled by the transportation of carbon dioxide in the concrete as well as the moisture condition in the concrete. The carbonation reaction needs some solution where the carbonation reaction can take place. This means that the carbonation rate is slow in dry concrete but increases in more moist concrete. In water-saturated concrete, the carbonation rate is slow due to slow transportation rate of carbon dioxide through the concrete. This was shown in a study performed by Glass et al. (1991). Usually, the propagation of a carbonation front can be seen if the pH-indicator phenolphthalein is added to the surface. The concrete surface turns pink if no carbonation has occurred (and is colourless if the surface is carbonated). A more detailed description of carbonation can be found in Bertolini, Luca. B Elsener, P Pedeferri (2004).

2.2 Strategies to decrease rebar corrosion

2.2.1 Type of concrete

A strategy to decrease corrosion of steel in concrete is to use concrete in which the time period needed to obtain the chloride threshold level is long. This may be achieved by e.g. using a thick concrete cover. Other methods are to use dense types of concretes with low water/cement (w/c) ratio and/or by adding additives such as micro silica which may decrease porosity, which decrease the chloride transportation rate. As an example, Manera et al. (2008) reported lower CTL for concrete with added silica fume compared with concrete without silica fume. Nowadays, several different cement types exist. The European standard EN 197-1(European commitee for standardisation 2000) distinguishes between cement types with different chemical composition. As an example in the European standard EN 206-1 (Standardization 2000) is it suggested that for concrete that is exposed to the splash/spray zone of seawater, the concrete should have w/c of 0.45 and a cement content of 340 kg cement by m^3 concrete.

Certain types of high performance concretes have a very fine pore structure. Yang (1999) suggested that the larger volume of very fine pores in high performance

concrete, increase the molar concentration of soluble ions which in turn decrease the RH.

2.2.2 Type of rebar material

By using more corrosion resistant materials such as stainless steel, the risk of corrosion can be decreased. This is due to that a more protective passive layer is formed on stainless steel compared to carbon steel, which means that higher chloride concentrations can be accepted within the concrete and possibly thinner concrete covers. Stainless steel contains minimum 12% chromium and the passive layer is very thin, about 2-3 nm and consists of protective chromium rich oxides. However the exact composition of the passive layer differs between different stainless steel qualities. Another benefit is that fully austenitic stainless steel is non-magnetic and can be used in constructions where magnetic materials such as carbon steel are not suitable. One drawback of using stainless steel rebar is that the cost is higher. García-Alonso et al. (2007) tested the stainless steel alloys AISI 304 and AISI 316 cast in mortar with 4% Cl and found no significant corrosion attack. Bertolini et al. (1996) showed that the superaustenitic alloy 254 SMO did not suffer of any localised corrosion in solutions with up to 10% Cl and temperatures up to 40 °C.

2.2.3 Inorganic and organic coatings for rebar

Inorganic layers on carbon steel such as galvanized carbon steel may be used in concrete. The zinc layer will act as a sacrificial anode and protect the rebar. During casting, the concrete is wet and the pH is high, which means that the corrosion rate of zinc is high. After hardening, the concrete is drier and the availability of oxygen is higher which means that the corrosion rate of zinc decreases. The corrosion rate of zinc depends on the composition of the corrosion products. Tittarelli & Moriconi (2010) showed that zinc can passivate in concrete if sufficient oxygen is available so that a layer of calcium hydroxyzincate is formed.

Several organic layer systems may be used on steel in concrete, e.g. systems based on epoxy, acrylic resin and polyurethane. The success of organic layers usually depends on the adhesion between the organic layer and the metal surface. Thick layers are generally more protective than thin layers. This was shown in a study by Swamy & Seiichi (1989) where an epoxy coating with three different thicknesses was applied on steel in concrete. Thicker coatings performed better when artificial damages was applied and exposed in an accelerated test. After three years of natural exposure no corrosion was found regardless of coating thickness. Generally, when organic coatings are damaged, blistering or delamination may occur. An important delamination

mechanism is cathodic delamination. This happens if the concentration of hydroxides increases between the organic layer and steel surface due to the cathodic reaction. More detailed information of deterioration mechanisms for organic layers can be found in Marcus (2012).

Duplex coatings made of a zinc layer on the steel surface and an organic coating on the zinc layer can be used. The benefit of using a duplex coating system is that even if the organic coating is damaged, the rebar will still be protected by the zinc layer underneath. The zinc layer is also protected by the high pH of the pore water. Dong et al. (2012) showed that a duplex coating system performs better than epoxy or galvanized steel alone.

A relative simple surface treatment which increases the corrosion resistance of steel in concrete may be to remove the mill scale on the steel surface. Silva (2013) compared steel with different surface conditions cast in concrete. It was reported that the susceptibility to corrosion was lower for chemically cleaned steel in acid compared to steel with the mill scale intact. Li & Sagues (2001) reported that sandblasted steel had higher corrosion resistance compared to steel with mill scale and pre-rusted steel in alkaline solutions. This may be explained by that crevices are formed between the mill scale and steel surface which are sites that are susceptible to corrosion. The mill scale is largely composed of magnetite with smaller amounts of wustite and hematite. Magnetite has about 10^{11} times higher electric conductivity compared to the other iron oxides which is stated in Cornell & Schwertmann (1996). It may be possible that crevice corrosion can propagate due to that electrons that are produced at the anodic site can be transported through the mill scale and reach the mill scale-concrete interface where the cathodic reaction takes place. The transportation of electrons through the mill scale is possible due to the high conductivity of magnetite. It has been reported by Lin et al. (2010) that chlorides are accumulated at anodic sites such as inclusions on the steel surface. These inclusions may be removed by pickling and thereby increase the corrosion resistance of the steel. This may explain why chemically cleaned steel surfaces perform better than steel surfaces with mill scale.

2.2.4 Cathodic protection

Cathodic protection means that the protected metal is polarized in a cathodic direction, meaning that anodic reactions on the surface are suppressed. This can be obtained by using sacrificial anodes or by impressed current. Sacrificial anodes were already discussed in 2.1.4 and here is only a brief description of impressed current.

A common way of using impressed current in concrete structures is to apply a net made of e.g. titanium on the concrete surface and thereafter cast a new layer of concrete over the surface. The titanium net is polarized in the anodic direction to a potential where the oxygen evolution reaction occurs. In concrete with high pH the anodic reaction will consume hydroxides and in concrete with lower pH the anodic reaction will consume water.

$4OH^- \rightarrow O_2 + 2H_2O + 4e^-$
$2H_2O \rightarrow O_2 + 4H^+ + 4e^-$

This means that the titanium is not consumed and the formed electrons are transported to the rebar, which is then protected. It is important that the impressed current is not so high that the rebar is cathodically polarized to potentials where hydrogen reduction occurs. If this happens, the formed hydrogen gas may cause hydrogen embrittlement of the steel. The formed hydrogen may also cause an acidification at the anode. To overcome this problem it is possible to lower the protection so that the steel is polarized to potentials where steel is passive and not immune. There may also be a risk of alkali-silica reactions due to an increased concentration of alkali at the rebar surface.

Koleva et al. (2007) investigated the concrete steel interface after cathodic protection with impressed current. The impressed current was between 5 and 20 mA/m^2 and the results showed a reduced salinity at the rebar and a more uniform and protective passive layer on the steel surface.

2.2.5 Other strategies

In addition to the already discussed strategies for decreasing the corrosion rate of rebar materials, a few more methods exist such as corrosion inhibitors which are mixed with the cement, or surface treatments such as hydrophobic and pore blocking treatments. Descriptions of these other methods can be found in Bertolini, Luca. B Elsener, P Pedeferri (2004)

3 Material and Methods

3.1 Laboratory exposure

3.1.1 Materials

The samples used in the laboratory exposure were made of steel cast in mortar. The mortar cover was about 5 mm and the composition of the steel is seen in Table 1, this type of steel was also used in the electrochemical experiments. The steel was cast in "as received condition" meaning that the pre-existing oxide scale was intact. Figure 3 shows the "cut off" surface of the oxide scale that is about 20-30µm thick. The composition of the mill scale is mostly magnetite and smaller amounts of wustite and hematite according to a XRD measurement. Before casting, the steel was degreased and thereafter immersed in a synthetic pore water solution to passivate. Poursaee & Hansson (2009) reported that it takes about three days for black steel to passivate in a pore solution with pH 13.3 and about seven days in OPC concrete.

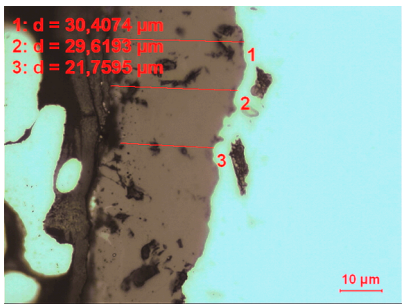

Figure 3. The cut off surface of the rebar with its mill scale, where the steel is to the right and the mill scale is measured.

The mortar was made with the following sand/cement/water mixture: 3/1/0.5 and the used cement was Portland cement CEM I("Anläggningscement", Cementa AB). Chlorides were added with the mixing water to obtain the following concentrations:

0, 0.2, 0.4, 0.6, 1.0, 1.5 and 2.0% Cl by mass of cement.

By adding chlorides to the mixing water, the pore structure may be altered. Suryavanshi et al. (1995) reported that when chlorides are added, the accessible pore volume decreases in OPC mortar compared to chloride free mortar. Moreover, the volume of finer pores increases and the volume of coarse pores decreases when chlorides are added.

Table 1 Chemical composition of the steel bar (% mass).

C	Mn	P	S	N	Cu
0.17	1.4	0.035	0.035	0.12	0.55

3.1.2 Exposure

The samples were exposed to static moisture conditions in dessicators with different relative humidities. Saturated salt solutions were placed at the bottom of each dessicator to produce the following relative humidities:

75, 85, 91, 93, 97 and 100% RH.

Samples were also exposed in a dynamic moisture condition, where samples were moved between an dessicator with 100% RH and an dessicator with 75% RH once a month.

Figure 4 shows an dessicator where the samples are standing above a saturated salt solution. To maintain stable moisture conditions a fan was mounted under the ceramic plate on which the samples were standing.

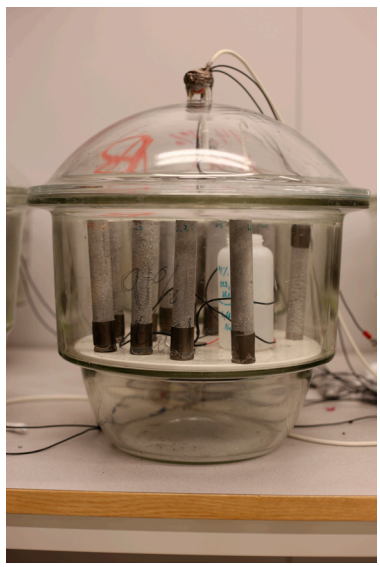

Figure 4. An example of an dessicator where the samples are standing on a ceramic plate and a fan is mounted under the plate. A saturated salt solution is placed at the bottom of the dessicator.

3.1.3 Measurements

The corrosion rate was measured with repeated pickling in Clarkes solution. During pickling, both corrosion products and the oxide scale are removed. Therefore, the corrosion rate was calculated by subtracting the mass loss of the oxide scale from the total mass loss of exposed steel. The mass of the mill scale was measured by pickling unexposed samples.

To check if the samples had obtained the wanted chloride concentrations, the chloride concentration was measured by SP-CBI (Swedish cement and concrete research institute) according to the following protocol. Mortar was crushed and about 1gram of powder was dissolved in dilute nitric acid heated to the boiling point. The solution was filtered and the chloride concentration was measured with a selective chloride ion electrode. The cement content was measured by titration with ethylenediaminetetraacetic acid (EDTA) and photometric measurement of the colour change with a murimex indicator. The cement content was obtained by assuming that the cement contained 63% CaO.

The capillary saturation of samples was measured according to:

$$S_{cap} = \frac{m_{sample} - m_{dry}}{m_{sat} - m_{dry}} \qquad (3)$$

Where m_{sample} is the mass of the sample, m_{dry} is the mass of samples after drying in 105°C, m_{sat} is the mass of sample after capillary saturation.

3.2 Electrochemical experiment

3.2.1 Experimental setup

For the electrochemical experiment, samples were made of steel cast in concrete. The composition of the steel can be seen in Table 1. The concrete cover was 50 mm and the w/c-ratio 0.5. After hardening the samples were immersed in a chloride containing solution and connected to a potentiostat. Stainless steel was used as counter electrode and Ag/AgCl as reference electrode.

The samples were polarized to the following potentials:

-100, -200, -300, -400, -500, -600, -700 and -800 mV vs. Ag/AgCl

The corrosion rate was measured by two different methods. The first method was by measuring the potential drop over a resistance and thereafter calculating the corrosion rate with Ohms law. In this way, the corrosion rate can be monitored over time. The second method, was by repeated pickling, as described in section 3.1.3. For comparison, the corrosion rate was calculated with and without the mill scale.

3.3 Field measurement

The corrosion potential of the rebar in the cooling water tunnel at a nuclear power plant was monitored during one year. The corrosion potential was logged and measured by using a reference electrode made of zinc. Figure 5 shows the potential logger mounted on the concrete wall. Zinc is useful as a reference electrode material due to its stable corrosion potential in seawater which is about -1017 mV vs SCE, stated in Baeckmann (1997).

Figure 5: The potential logger mounted on the concrete wall is shown to the left and an sacrificial anode mounted on the concrete wall is shown to the right.

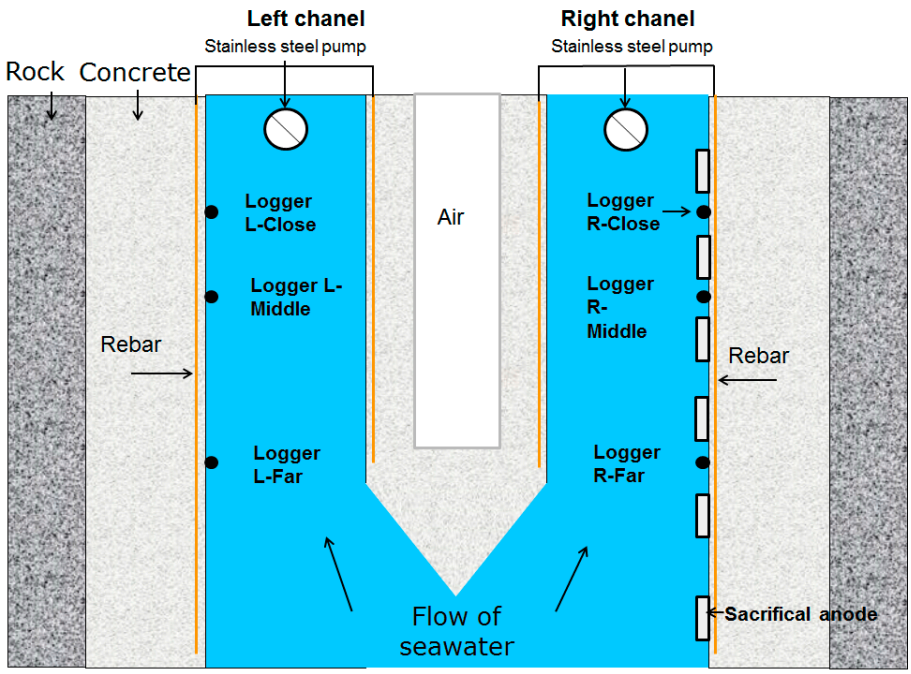

Figure 6. A schematic figure of the cooling water tunnel, where sacrificial anodes were mounted in the right tunnel. Water pumps made of stainless steel were installed in the ceiling at the end of each tunnel.

The cooling water tunnel is divided into a left tunnel and a right tunnel, see Figure 6. Sacrificial anodes were mounted on the right tunnel whereas no sacrificial anodes were mounted in the left tunnel. The sacrificial anodes were made of an Al-In alloy and figure 5 shows an example of an anode mounted to the concrete wall. Three potential loggers were mounted in each tunnel and the potential was monitored during one year. Water pumps made of stainless steel were installed in the ceiling at the end of each tunnel. The reason why the potential loggers were installed at different distances from the pumps was to assess if the measured potential decreased with a longer distance from the pumps.

4 Results and Discussion

4.1 Rebar corrosion dependency of moisture condition

4.1.1 Static moisture condition

Samples exposed to high RH weighed more compared to samples exposed to lower RH. The higher weight is because more capillary condensed water is formed in the mortar, which means that the capillary water saturation increases. Samples with high chloride content also weighed more compared to samples with lower chloride content at the same RH exposure. This is due to the fact that chlorides are hygroscopic, which means that more capillary condensed water is formed. An example of how much chlorides increase the capillary water saturation can be seen in Figure 7, where samples with different chloride content are exposed to 75% RH. Samples with no chlorides had a capillary saturation of 0.5 and for samples with 2% Cl the capillary saturation was about 0.75.

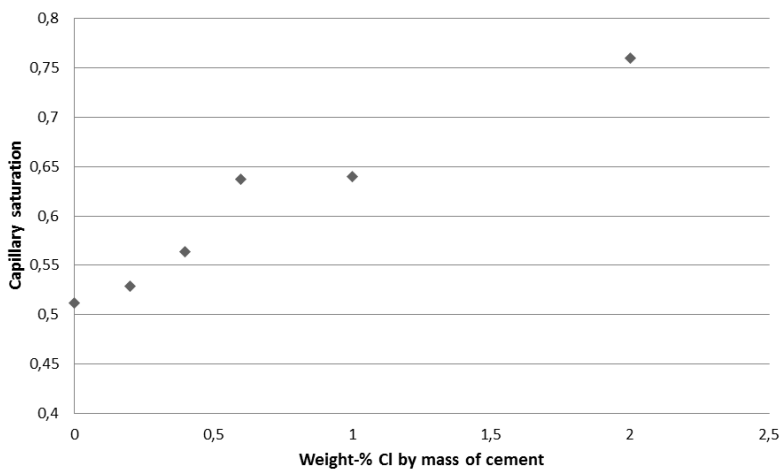

Figur 7: The capilary saturation of samples with different chloride concentrations exposed to 75% RH.

Samples were exposed to different static RH conditions and the corrosion rate was measured after a short exposure period (about 3 months) and a longer exposure period (about 15 months). The average corrosion rate of samples for the short exposure period can be seen in Figure 8. For samples with low chloride content (0.2-1.0% Cl), corrosion had not been initiated regardless of moisture condition. For samples with high chloride content (1.5-2.0% Cl), corrosion had been initiated and a maximum corrosion rate could be seen for samples exposed in 90-93% RH. The corrosion rate decreased when the RH was outwith this interval. This is due to that when samples are exposed to lower RH, the resistivity of the mortar decreases, and for samples exposed to higher RH, the samples are nearly capilary saturated.

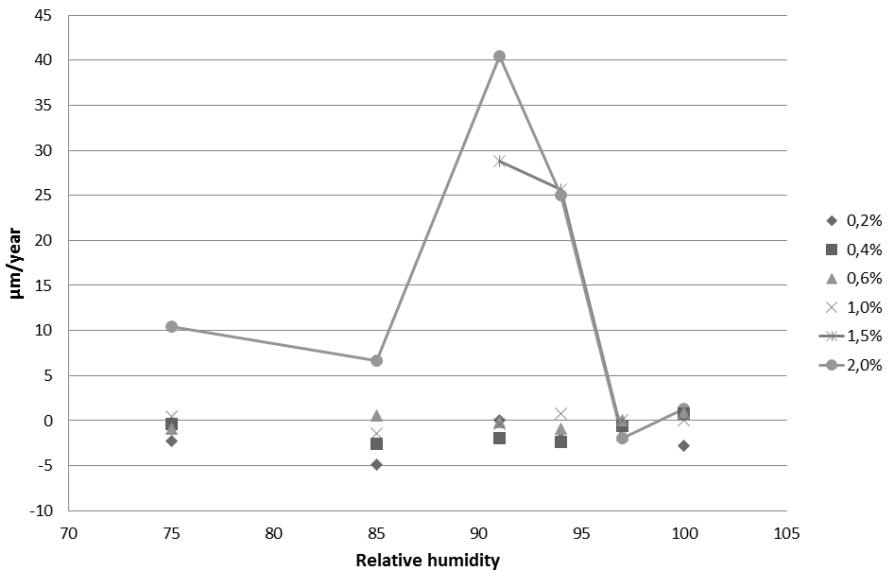

Figure 8. The corrosion rate of samples with different chloride concentrations (% Cl by mass of cement) exposed to different RH after approximately 3months exposure. The corrosion rate was calculated after subtraction of the pre-existing mill scale.

The corrosion rate of samples during the long exposure period can be seen in Figure 9. The highest corrosion rate was obtained at 97% RH for samples with low Cl content (0.2-1.0% Cl). This means that the maximum corrosion rate is obtained at higher moisture conditions for samples with low chloride content compared to samples with high chloride content. This is probably due to that the samples with low chloride content need a higher moisture content to decrease the resistivity to obtain corrosion maximum. This also suggests that the present measurements should be complemented with measurements at even higher RH levels than 97% to verify the CTL.

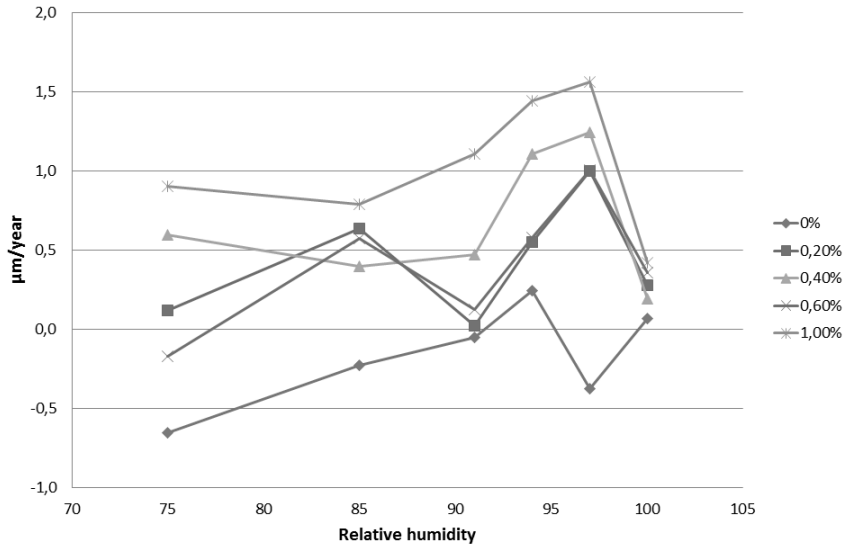

Figure 9. Corrosion rates of samples with chloride concentrations from 0 to 1.0% Cl by mass of cement exposed to different relative humidity after approximately 15 months exposure. The corrosion rate was calculated after subtraction of the pre-existing mill scale.

The steel surface after exposure in mortar with 1% Cl and 97% RH is seen in Figure 10. It can be seen that the mill scale has been lifted from the steel surface due to formation of corrosion products under the mill scale. These formed corrosion products caused cracking in the mortar cover. From the results presented here, the CTL is lower than 1% Cl by mass of cement for steel in mortar exposed to static moisture conditions.

Generally, the results in this study are relatively similar to previously reported results. It has been shown that when steel in mortar is exposed to low RH, the corrosion rate is low due to high resistivity. When steel in mortar is exposed to high RH the corrosion rate is also low due to slow transportation rate of oxygen. At an intermediate RH level, the corrosion rate is high due to relatively low resistivity and fast transportation rate of oxygen. Tuutti (1982) exposed samples made of steel in mortar with one high chloride concentration to different relative humidities. The highest corrosion rate was found at 95% RH which can be compared with the samples with 2% Cl in the present study where a corrosion maximum was found at about 91% RH. This relatively small RH difference may be explained by that the previous study used a more porous mortar (w/c 0.7) which means a faster transportation rate of oxygen and subsequently faster initiation.

Pettersson (1997) exposed samples made of steel in mortar to different RH levels and measured the corrosion rate with LPR. The CTL was reported to be 0.5%

Cl measured at 90% RH. Higher chloride concentrations were needed to initiate corrosion at higher or lower RH levels than 90%. The lower reported CTL value compared to this study (CTL lower than 1.0% Cl at 97% RH) may be explained by the difficulties of measuring a corrosion rate of steel in concrete at different moisture conditions, as suggested by Millard et al. (2001). Another explanation may be that a steel surface in concrete can activate and passivate several times before a stable corrosion pit is formed which was reported by Angst el al. (2011). It is therefore possible that the first activation was measured with LPR that resulted in a low reported CTL value. A higher reported CTL value would have been reported if the CTL value were corresponding to a stable pit formation.

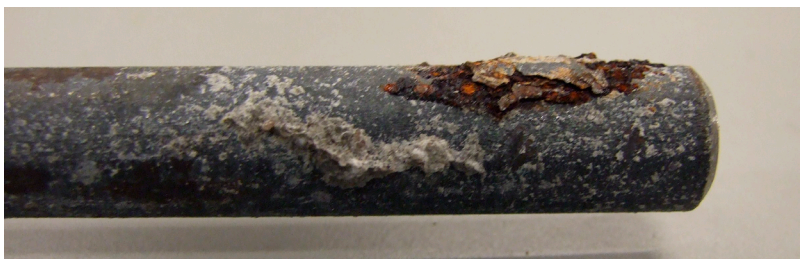

Figure 10: The surface of a steel sample cast in mortar with 1% Cl by mas of cement exposed to 97% RH. The figure shows that a part of the mill scale is detached from the steel surface probably due to formed corrosion products beneath the mill scale.

To check if the desired chloride concentration was obtained during casting, the chloride concentration in the mortar was measured in the laboratory after exposure. It was concluded that the desired and measured chloride concentration was similar for samples with chloride concentrations up to 1.0% Cl. For samples with higher chloride concentrations the correlation was less good. As an example, samples exposed in 97% RH with the desired 2% Cl concentration were measured to have 1.3% Cl. This is significantly lower than the desired concentration. At the same time, samples with the desired 2% Cl exposed in 75% Cl the measured concentration was 1.8% Cl. It was therefore suggested that chlorides were leaking out from samples with high chloride concentrations exposed to high RH.

4.1.2 Dynamic moisture condition

The corrosion was measured to be higher for samples exposed in dynamic moisture conditions when compared to static moisture conditions. Corrosion was initiated for samples with chloride concentrations between 0.4 and 0.6% Cl. This may have several explanations. One explanation is that the optimum moisture condition is obtained somewhere between 75-100% RH where corrosion is more easily initiated. It may also be possible that chlorides are more easily accumulated at anodic sites due to an ongoing transport of moisture. Another explanation is that small cracks are

formed due to the dynamic moisture flow, this was shown in a numerical study performed by Jankovic & van Mier (2001). Gran & Hansen (1997) showed that the pore structure coarsens during drying. This may also form cracks during moisture cycling due to repeated changes of the pore structure. The cracks formed may increase the transportation rate of moisture and oxygen, which would increase the corrosion rate.

Figure 11. Corrosion products formed on the steel in mortar with 0.6% Cl exposed to dynamic moisture conditions.

One last explanation is that the mortar is carbonated so the pH of the pore water at the steel surface is low. To assess if carbonation was ongoing, phenoftalein was added on the mortar surfaces which turned pink. Therefore, the relatively high corrosion rates are not due to carbonation. Figure 11 shows the steel samples cast in 0.6% Cl and exposed in dynamic moisture conditions. The average corrosion rate for these samples was 2.1 μm/year.

4.2 Rebar corrosion in water saturated concrete

4.2.1 Electrochemical experiment

To assess at which potentials corrosion is initiated for steel in concrete, samples were polarized to various potentials. The samples had 1 or 2% Cl and the corrosion current was measured over a relatively long time, between 20 and 100 days depending on polarization. The corrosion rate for samples with 2% Cl can be seen in Figure 12. Corrosion was initiated at -400mV vs. SCE for samples with 2% Cl and about -100mV for samples with 1% Cl. It was therefore concluded that the risk of corrosion increases when the corrosion potential is more anodic than -500 mV vs SCE for steel in concrete with 2% Cl and about -200 mV for steel in concrete with 1% Cl. The measured corrosion rates were similar from the current measurement and the pickling measurement. The calculated corrosion rate without the mill scale was lower compared to the other corrosion rates. This may suggest that the measured current is divided into a faradaic current and a non-faradaic current. The faradaic current is oxidation of iron and the non-faradaic current is from other

reactions taking place in the mill scale. (Alonso et al. 1998) suggested that magnetite in the mill scale may transform into maghemite during anodic polarization. This reaction would produce electrons and a non-faradaic current.

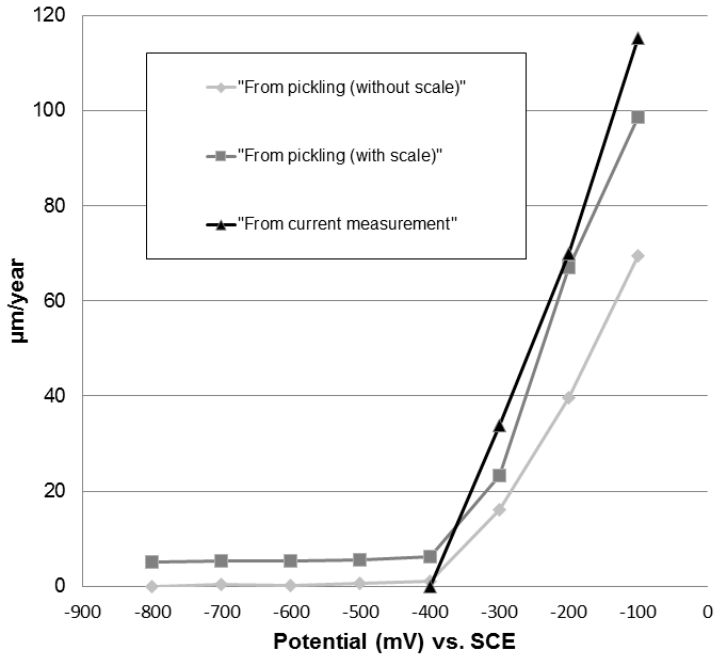

Figure 12. Corrosion rate for sample with 2% Cl by mass of cement. Corrosion rate is measured by repeated pickling calculated with and without the mill scale and calculated from the average corrosion current during polarization.

4.2.2 Field study

The potentials measured during one year in the cooling water tunnels can be seen in Figure 13, see also Figure 6 for positions of the loggers. The potential loggers were mounted on the concrete at different distances from the stainless steel pumps. Sacrificial anodes were mounted in the right tunnel and it has been reported that the consumption rate of the anodes is unexpectedly rapid.

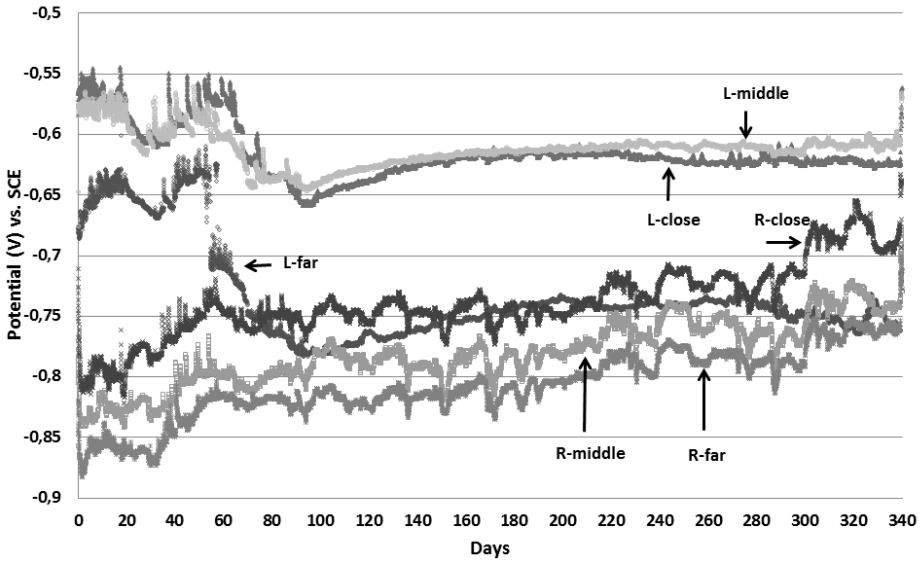

Figure 13. The potentials measured in the right and left tunnel, where R-close, R-middle, R-far, are the potentials in the right tunnel at different distances from the pumps. L-close, L-middle, L-far are the potentials in the left tunnel at different distances from that pumps. Close means close to the pumps and far means far from the pumps.

The measured potentials in the right tunnel were generally lower than the potentials in the left tunnel due to the mounted sacrificial anodes. This means that the sacrificial anodes are protecting the rebar in the right tunnel. Rebar is generally fully protected when the corrosion potential is lower than -800 mV vs. SCE according to Anon (2010). This potential level was obtained in the beginning of the measurements but thereafter, the potential was slowly shifted to more anodic potentials. The reason why the potentials were increasing with time is not known. One possible explanation is that chlorides are transported away from the rebar due to the cathodic protection, as discussed in 2.1.4. During the measurements, the temperature of the seawater was fluctuating between -1 and 20°C. This means that the water temperature should in principle affect the measured potentials due to temperature dependent resistivity and oxygen concentration but no such correlation could be made. The potentials in the right tunnel were also shifted to more positive potentials when the distance to the pumps decreased. This means that the pumps were affecting the potential of the rebar and this may explain the rapid consumption rate of the sacrificial anodes. The potentials in the left tunnel were more anodic than the potentials in the right tunnel except for the potential measured with the logger L-far. L-far was the logger which was mounted at the longest distance from the pumps compared to the other loggers in the left tunnel. The potential decreased to the same potential region as in

the right tunnel. The reason for the decreased potential is that the sacrificial anodes on the right side were affecting the potential logger on the left side.
The electrochemical study above concluded that the risk of corrosion increases when the measured potential is more anodic that -500 mV vs SCE for steel in concrete with 2% Cl. The measured potentials in the left and right tunnel were not as anodic as the potential where the risk of corrosion increases. The chloride concentration of drilled concrete core samples was measured to be lower than 1% Cl which should mean that the risk of corrosion increases at potentials higher than -200 mV. However, due to the fact that the measured potentials increased with shorter distance to the pumps, and that the potential was not measured in the very vicinity of the pumps, the risk of corrosion cannot be discarded for the concrete in the very vicinity to the pumps.

5 Conclusions

This study assessed corrosion of steel in mortar at various chloride and humidity levels and the main conclusions are given below.

- Exposures in constant RHs from 75% to 100% show that the corrosion rate is moisture dependent with a maximum in the interval 91% to 97% depending on the chloride concentration. In the present study, the chloride threshold level was measured to be 1% Cl by mass of cement measured at 97% relative humidity.
- At higher chloride concentration (2%) the maximum is at the lower end of this RH interval while at lower chloride concentrations (0.1% to 1.0%) the maximum is at the higher end of this interval. The interpretation of the maximum corrosion rate is that below the respective relative humidity there is a resistive control while above the maximum the high water content results in a limitation of oxygen transport. This suggests that chloride threshold levels should be evaluated at rather humid conditions (97%) despite the fact that the maximum corrosion rate at higher chloride levels is observed in the interval 91% to 94%.
- For cyclic moisture conditions between 75% and 100% RH the corrosion rate at 0.6% chloride was considerably higher than the maximum value obtained at 97% RH static conditions, the most corrosive RH value. This suggests that there is an overestimation of chloride threshold levels evaluated from exposures performed at stationary conditions.
- The rapid consumption of the sacrificial anodes is mainly explained by the connection between the rebar in concrete and the stainless steel pumps. The stainless steel pumps have a relatively noble potential and together with a high flow rate this will lead to an increased anodic current from the sacrificial anodes.
- The steel reinforcement close the stainless steel pumps has a higher risk of galvanic corrosion compared to the steel bars situated at longer distances from the pumps.

6 Future Research

In this study it was concluded that the lowest chloride threshold level was found at 97% RH. However, the RH levels between 97% and 100% RH were not included and this moisture interval may be an optimum for corrosion where the resistivity is low and the oxygen diffusion is relatively high. Corrosion of steel in mortar should therefore be assessed at 97-100% RH.

It has been suggested that the use of fly ash and granulated blast furnace slag in concrete production will increase in the future. The corrosion dependence to different moisture conditions in these types of concretes should also be investigated.

The chloride threshold level in dynamic moisture condition was lower compared to in static moisture condition. The mechanisms behind this behaviour are not known. One explanation may be that an optimium moisture condition is obtained. Another is that cracks are formed due to moisture cycling or that the ongoing transportation of moisture also increases transportation of other substances. Therefore, the corrosion behaviour of steel in mortar exposed to dynamic moisture conditions should be investigated further.

The most commonly used rebar material has a mill scale on the surface. Different chemical compositions of the mill scale will probably have different properties which affect initiation of corrosion. It might be possible that crevices are formed between the mill scale and the steel surface. Crevice corrosion can propagate due to the high electrical conductivity of magnetite. Therefore, would it be interesting to investigate the corrosion properties of steel with different surface characteristics such as with a mill scale and cleaned steel by blasting and acid.

7 Reference List

Abreu, C., Cristóbal, M. & Montemor, M., 2002. Galvanic coupling between carbon steel and austenitic stainless steel in alkaline media. *Electrochimica 47*, pp.2271–2279. Available at: http://www.sciencedirect.com/science/article/pii/S0013468602000865 [Accessed March 26, 2013].

Alonso, C., Andrade, C. & Novoa, X., 1998. Effect of protective oxide scales in the macrogalvanic behaviour of concrete reinforcements. *Corrosion science*, 40(8), pp.1379–1389. Available at: http://www.sciencedirect.com/science/article/pii/S0010938X98000407 [Accessed March 26, 2013].

Alonso, C., Castellote, M. & Andrade, C., 2002. Chloride threshold dependence of pitting potential of reinforcements. *Electrochimica acta*, (47), pp.3469–3481.

Angst, U. et al., 2009. Critical chloride content in reinforced concrete — A review. *Cement and Concrete Research*, 39(12), pp.1122–1138. Available at: http://linkinghub.elsevier.com/retrieve/pii/S0008884609002099 [Accessed November 14, 2012].

Angst, U.M. et al., 2011. Chloride induced reinforcement corrosion : Electrochemical monitoring of initiation stage and chloride threshold values. *Corrosion Science*, 53(4), pp.1451–1464. Available at: http://dx.doi.org/10.1016/j.corsci.2011.01.025.

Anon, 2010. Cathodic protection design, Recommended practice. Det norske veritas, DNV-RP-B401.

Baeckmann, W. von, 1997. *Handbook of Cathodic Corrosion Protection* third edit., Gulf publishing company. Available at: http://cdsweb.cern.ch/record/1085921.

Bertolini, L. et al., 1996. behaviour of stainless steel in simulated concrete pore solution.pdf. *British corrosion journal*.

Bertolini, Luca. B Elsener, P Pedeferri, R.P., 2004a. *Corrosion of steel in concrete - Prevention, Diagnosis, Repair* first edit., Weinheim: Wiley-Vch.

Bertolini, Luca. B Elsener, P Pedeferri, R.P., 2004b. Corrosion of steel in concrete. Prevention, diagnosis, repair.

Cornell, R.M. & Schwertmann, U., 1996. *The Iron Oxides*, Wiley-VCH.

Dong, S. et al., 2012. Corrosion behavior of epoxy/zinc duplex coated rebar embedded in concrete in ocean environment. *Construction and Building Materials*, 28(1), pp.72–78. Available at: http://linkinghub.elsevier.com/retrieve/pii/S0950061811004594.

European commitee for standardisation, 2000. EN 197-1 "Cement part1: Composition, specifications and conformity criteria for common cements."

García-Alonso, M.C. et al., 2007. Corrosion behaviour of new stainless steels reinforcing bars embedded in concrete. *Cement and Concrete Research*, 37(10), pp.1463–1471. Available at: http://linkinghub.elsevier.com/retrieve/pii/S0008884607001305.

Ghods, P. et al., 2010. Electrochemical investigation of chloride-induced depassivation of black steel rebar under simulated service conditions. *Corrosion Science*, 52(5), pp.1649–1659. Available at: http://linkinghub.elsevier.com/retrieve/pii/S0010938X10000752.

Glass, G.K. & Buenfeld, N.R., 1997. The presentation of the chloride threshold level for corrosion of steel in concrete. *Corrosion Science*, 39(5), pp.1001–1013. Available at: http://linkinghub.elsevier.com/retrieve/pii/S0010938X97000097.

Glass, G.K., Page, C.L. & Short, N.R., 1991. Factors affecting the corrosion rate of steel in carbonated mortars. *Corrosion Science*, 32(12), pp.1283–1294. Available at: http://linkinghub.elsevier.com/retrieve/pii/0010938X9190048T.

Gran, H.C. & Hansen, E.W., 1997. Effects of drying and freeze thaw cycling probed by H-NMR. *Cement and concrete reasearch*, 27(9), pp.1319–1331.

Hausmann, D.A., 1967. Steel corrosion in concrete. *Materials protection*, 6(19).

Hornbostel, K., Larsen, C.K. & Geiker, M.R., 2013. Relationship between concrete resistivity and corrosion rate – A literature review. *Cement and Concrete Composites*, 39, pp.60–72. Available at: http://linkinghub.elsevier.com/retrieve/pii/S0958946513000383.

Jankovic, D. & van Mier, J.G.M., 2001. Crack development in concrete due to moisture flos. *Heron*, 46.

Koleva, D. a. et al., 2007. Investigation of Corrosion and Cathodic Protection in Reinforced Concrete. *Journal of The Electrochemical Society*, 154(5), p.C261. Available at: http://link.aip.org/link/JESOAN/v154/i5/pC261/s1&Agg=doi.

Li, L. & Sagues, A.A., 2001. Chloride corrosion threshold of reinforcing steel in alkaline solutions - Open circuit immersion tests. *Corrosion*, 57(1), pp.19–28.

Lin, B. et al., 2010. A study on the initiation of pitting corrosion in carbon steel in chloride-containing media using scanning electrochemical probes. *Electrochimica Acta*, 55(22), pp.6542–6545. Available at: http://linkinghub.elsevier.com/retrieve/pii/S0013468610008273.

Lopez, W. & Gonzalez, J.A., 1993. Influence of the degree of pore saturation on the steel resistivity of concrete and the corrosion rate of steel reinforcement. *Cement and concrete reasearch*, 23, pp.368–376.

Manera, M., Vennesland, Ø. & Bertolini, L., 2008. Chloride threshold for rebar corrosion in concrete with addition of silica fume. *Corrosion Science*, 50(2), pp.554–560. Available at: http://linkinghub.elsevier.com/retrieve/pii/S0010938X07002223.

Manouchehr Hassanzadeh, 2014. *REPARATION AV BETONGKONSTRUKTIONER Skador och reparationsmetoder från 1970-talet och framåt Reparationsbehov , forskningsbehov , effektivitet TVBM-3176*, (in swedish)

Marcus, P., 2012. *Corrosion Mechanisms in Theory and Practice* P. Marcus, ed., CRC Press. Available at: http://www.crcnetbase.com/doi/book/10.1201/9780203909188.

Melchers, R.E. & Li, C.Q., 2009. Reinforcement corrosion initiation and activation times in concrete structures exposed to severe marine environments. *Cement and Concrete Research*, 39(11), pp.1068–1076. Available at: http://linkinghub.elsevier.com/retrieve/pii/S000888460900163X.

Michel, A., Nygaard, P.V. & Geiker, M.R., 2013. Experimental investigation on the short-term impact of temperature and moisture on reinforcement corrosion. *Corrosion Science*, 72, pp.26–34. Available at: http://linkinghub.elsevier.com/retrieve/pii/S0010938X13000784.

Millard, S.G. et al., 2001. Environmental influences on linear polarisation corrosion rate measurement in reinforced concrete. *NDT&E International*, 34, pp.409–417.

Nasser, A. et al., 2010. Influence of steel–concrete interface condition on galvanic corrosion currents in carbonated concrete. *Corrosion Science*, 52(9), pp.2878–2890. Available at: http://linkinghub.elsevier.com/retrieve/pii/S0010938X10002246.

Parthiban, G.T. et al., 2008. Cathodic protection of steel in concrete using magnesium alloy anode. *Corrosion Science*, 50(12), pp.3329–3335. Available at: http://linkinghub.elsevier.com/retrieve/pii/S0010938X08003387 [Accessed June 19, 2012].

Pettersson, K., 1997. *Service life of concrete structures in a chloride environment. Report 1:97*, Stockholm.

Poursaee, a. & Hansson, C.M., 2009. Potential pitfalls in assessing chloride-induced corrosion of steel in concrete. *Cement and Concrete Research*, 39(5), pp.391–400. Available at: http://linkinghub.elsevier.com/retrieve/pii/S000888460900026X.

Sandberg, P., 1999. Studies of chloride binding in concrete exposed in a marine environment. 29(February 1998), pp.473–477.

Sederholm, B. & Selander, A., 2011. *Katodiskt skydd av betongkonstruktioner med termiskt sprutade offeranoder av zink Katodiskt skydd av betongkonstruktioner med termiskt sprutade offeranoder av zink*, Elforsk rapport 11:55 (in swedish)

Silva, N., 2013. *Chloride Induced Corrosion of Reinforcement Steel in Concrete Threshold Values and Ion Distributions at the Concrete-Steel Interface Department of Civil and Environmental Engineering Chloride Induced Corrosion of Reinforcement Steel in Concrete*, Phd thesis, Chalmers University

Standardization, E. commitee for, 2000. En 206-1 "Concrete part 1: Specification, performance, production and conformity." , pp.1–72.

Suryavanshi, A.K., Scantlebury, J.D. & Lyon, S.B., 1995. Pore size distribution of OPC and SRPC mortars in presence of chlorides. *Cement and concrete reasearch*, 25(5), pp.980–988.

Swamy, R.N. & Seiichi, K., 1989. Epoxy Coated Rebars The Panacea for Steel Corrosion in Concrete. *Construction and Building Materials*, 3, pp.86–91.

Tittarelli, F. & Moriconi, G., 2010. The effect of silane-based hydrophobic admixture on corrosion of galvanized reinforcing steel in concrete. *Corrosion Science*, 52(9), pp.2958–2963. Available at: http://linkinghub.elsevier.com/retrieve/pii/S0010938X10002465.

Tuutti, K., 1982. *Corrosion of steel in concrete*. Swedish cement and concrete research intitute. Available at: http://trid.trb.org/view.aspx?id=194388.

Yang, Q., 1999. Inner relative humidity and degree of saturation in high-performance concrete stored in water or salt solution for 2 years. *Cement and Concrete Research*, 29(1), pp.45–53. Available at: http://linkinghub.elsevier.com/retrieve/pii/S0008884698001744.

Paper I

Galvanic corrosion properties of steel in water saturated concrete

J. Ahlström*, J. Tidblad, B. Sandberg and L. Wadsö

Aluminum-based sacrificial anodes were installed to reinforced concrete to stop ongoing corrosion in cooling water tunnels in a Swedish nuclear power plant. The steel rebars were also unintentionally connected to stainless steel water pumps. Therefore, the consumption rate of the sacrificial anodes was higher than predicted. An experimental and a field study were performed to assess if the steel rebar suffer from galvanic corrosion and if the stainless steel pumps are responsible alone for the high consumption rate. It was found from the experimental study that there is an increased risk of galvanic corrosion for steel rebar when the corrosion potential is raised to −200 mV (SCE) for samples with 1% Cl^- by mass of cement and −500 mV (SCE) for samples with 2% Cl^- by mass of cement. The experimental results were compared with the corrosion potential measured in the cooling water tunnel where sacrificial anodes were in use and not mounted at all. The cooling water tunnel without sacrificial anodes had generally more anodic corrosion potentials compared to the tunnel with anodes. The tunnel with anodes had also more anodic potentials closer to the stainless steel pumps than further away which means that the rebar is affected by the stainless steel pumps. However, the measured corrosion potentials in the tunnels were not as anodic as the potentials needed for high galvanic current measured in the experimental study.

1 Introduction

Steel is normally passive in concrete with low chloride concentrations due to the high pH of the pore water solution. Corrosion damage of structures made of concrete is mostly reported from environments where chlorides are transported through the concrete cover to the steel and where the moisture content is high enough to allow ion transport, but still low enough to allow oxygen transport. In water saturated concrete corrosion, damage is normally not seen due to the slow oxygen transport to the steel surface. However, the resistivity of water-saturated concrete is relatively low and if a rebar is connected to a more noble material there is a risk of galvanic corrosion. If the rebar and the noble material are cast within the same concrete structure the galvanic current will be relatively small due to the low rate of oxygen transport resulting in lower oxygen concentration. A high galvanic current is more likely if the noble material is situated in the water outside the concrete structure where both the oxygen concentration and the transport rate are higher.

Galvanic corrosion of carbon steel rebar connected to stainless steel rebar has been studied in alkaline solution by Ref. [1] and in concrete by Ref. [2]. These studies suggest that there is not an increased risk of galvanic corrosion when carbon steel is connected to stainless steel in concrete. In fact, a higher macrocell current was measured when passive carbon steel was connected to active carbon steel in concrete. Concrete structures in chloride containing environments are said to start corroding when the critical chloride threshold level is reached. Several different studies have been performed trying to establish this critical chloride concentration but the reported results have high variations. An excellent review of reported critical threshold levels and general corrosion properties for steel in concrete can be found in Ref. [3]. Only few field studies of chloride thresholds have been conducted, which possibly is a problem as accelerated laboratory tests may propose low chloride threshold concentrations. *Sandberg* [4] performed a large study of chloride-initiated corrosion in concrete exposed in a marine environment. His results showed that the chloride threshold level for concrete slabs (with water/binder ratio of 0.5 exposed in the splash zone) was between 0.6 and 1.2% chloride by mass of binder.

Swedish nuclear power plants use seawater as cooling water, which is transported through concrete channels. The cooling

J. Ahlström, J. Tidblad, B. Sandberg
Swerea KIMAB, Isafjordsgatan 28A, 164 40, Kista, (Sweden)
E-mail: johan.ahlstrom@swerea.se

L. Wadsö
Division of Building Materials, Lund University, Box 118, SE-22100, Lund, (Sweden)

water tunnels are thus important parts of these nuclear power plants. In a particular case, it was observed that Al–Zn–In sacrificial anodes connected to the rebars had been consumed more rapidly than originally predicted. Furthermore, it was found that the rebars were unintentionally electrically connected to the stainless steel water pumps. This study was to investigate if the stainless steel water pumps were responsible for the high consumption of the sacrificial anodes and if there is a risk that the rebars suffer from galvanic corrosion. The galvanic corrosion properties of the steel in concrete were assessed under both laboratory and field conditions. Electrochemical experiments were performed to investigate at which potentials, steel in concrete may suffer from galvanic corrosion. The corrosion potential of the rebar in a cooling water tunnel was measured in the field study and compared with the potentials from the electrochemical experiments to make a complete analysis of the galvanic corrosion properties of steel in water saturated concrete.

2 Experimental

2.1 Electrochemical experiments

The carbon steel composition of the alloy used in the electrochemical experiments, S235JR (SS-EN 10025-2:2004), is shown in Table 1. The steel bars had a diameter of 12 mm and were cut into 150 mm lengths. The surface of the steel bars was smooth and in an as-received condition with the oxide scale intact. Before casting, the steel bars were degreased with trichlorethylene. The degreasing procedure was 30 s in steam followed by 5 min in an ultrasound bath. This procedure was repeated four times. A connector was attached to the end of the rebar and covered with heat shrink tubing with melt glue over the connection. The length of the exposed rebar (without shrink tubing) was 60 mm. The steel was cast in mortar with Portland cement and sand (<4 mm). The water/cement ratio was 0.6 and the concrete cover 60 mm. Sodium chloride was added with the mixing water to produce concrete samples with 1 and 2% Cl^- by mass of cement. The concrete samples were cured in 100% relative humidity for 28 days. A schematic picture of the experimental set-up is seen in Fig. 1.

A cylindrical tube made of stainless steel, EN 1.4436, was used as counter electrode. The working electrode, i.e. the rebar casted in the cylindrical concrete sample, and a reference electrode was placed close to the concrete sample. The reference electrode was either an Ag/AgCl sat. KCl or a saturated calomel electrode (SCE) (the Ag/AgCl type electrode was corrected by 50 mV so that all presented potentials are with reference to a SCE electrode). The electrodes were immersed in a 3% NaCl test solution for samples with 1% Cl^- and 6% NaCl test solution for samples with 2% Cl^- by mass of cement. These ion solute concentrations approximately correspond to the chloride concentration in the specimens [5]. The surface of the test solution was kept at a level just under the top of the concrete sample. The steel rebars in concrete were potentiostatically polarized to potentials between −100 and −800 mV *versus* SCE. Only one concrete sample was polarized at each potential and the measured corrosion rate is therefore only a rough estimation. Additionally, unpolarized samples with 1 and 2% Cl^- were exposed in the respective test solution. The corrosion rate of the unpolarized samples was measured over time. The potentiostat used for each concrete sample was a Sycopel Ministat. The corrosion current was measured by measuring the potential drop over a resistance.

Table 1. Chemical composition of steel bar (% in mass)

C	Mn	P	S	N	Cu
0.17	1.4	0.035	0.035	0.12	0.55

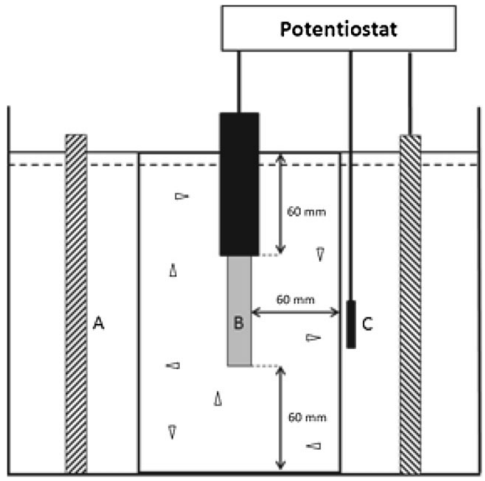

Figure 1. Experimental test set-up showing the cylindrical tube made of stainless steel as counter electrode, (A), the steel rebar in concrete as a working elektrode, (B), and a reference electrode, (C)

The average corrosion rate was measured by repeated pickling in Clark's solution containing per liter: 20 g Sb_2O_3, 60 g $SnCl_2$, and 1 L HCl 37%. As the steel was exposed in an as-received condition, the oxide scale present already before exposure is also removed from the steel surface during pickling and contributes to the total measured mass loss. Therefore, unexposed samples were also pickled to quantify the average weight and thickness of the oxide scale. In order to report a correct corrosion rate it is necessary to subtract the mass loss from the preexisting oxide scale from the total weight loss of exposed samples.

2.2 Field study

The corrosion potential of the rebar unintentionally connected in a cooling water tunnel was measured when connected with stainless steel water pumps in flowing seawater. The cooling water tunnel has been in use since 1983, when the reactor started. The main cooling water tunnel is divided into a left and right channel as seen in Fig. 2. The concrete wall on the right side of the right channel is opposite to rock and the left side of the right

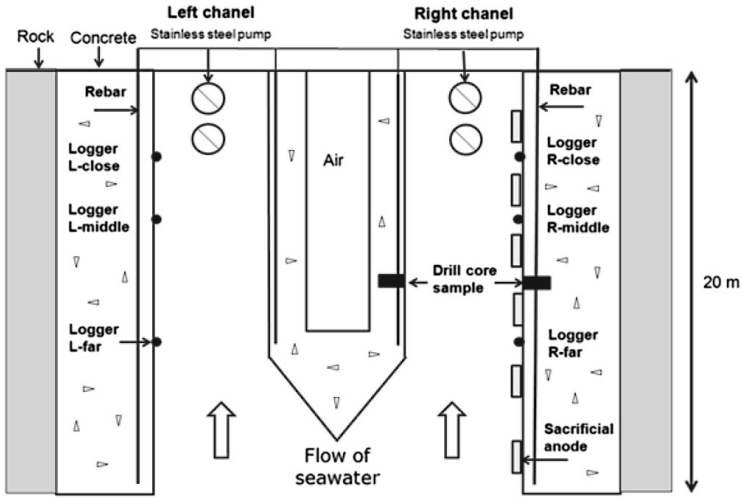

Figure 2. Schematic figure of the cooling water tunnel as seen from above. The main cooling water tunnel is divided into a left and a right channel. The rebar on the right side of the right channel is connected to sacrificial anodes made of an Al–Zn–In alloy. The stainless steel pumps are mounted into the ceiling and pump the water upwards. A combined reference electrode and data logger devices were connected to the rebar at different distances to the pumps in the left and right channel. Drill core samples were taken from the wall opposite to air and rock in the right channel

channel is opposite to air. The rebar on the right side is connected to sacrificial anodes made of an Al–Zn–In alloy. The stainless steel pumps are mounted into the ceiling at the end of the right and left tunnel. As seen in Fig. 2, the exterior concrete walls of both tunnels were cast against rock, while the concrete structure between the two tunnels contains an inspection tunnel/room/cavity (air). The rebar on the left side is not connected to sacrificial anodes. The reinforcement was connected at several points as indicated in Fig. 2 to combined reference electrode and datalogger devices (nke instrumentation) where zinc rods were used as a reference electrodes. Zinc has very stable potential in seawater (−1017 mV *vs.* SCE) [6]. The potential and the seawater temperature were measured and stored in each logger at 10 min intervals. Unfortunately, it was not possible to reach the stainless surfaces in the pumps, which were in contact with seawater. Therefore, the corrosion potential of the stainless steel pumps could not be measured.

The concrete quality used for the cooling water tunnels were equivalent to today's C25/C30 standard. The cement was Gullhögens LH, a slow hardening Portland cement and the water/cement ratio (W/C) was 0.6. The concrete cover of the walls was 50 mm. Drill core concrete samples were collected from the right channel's walls as marked in Fig. 2. The concrete samples were analyzed with respect to chloride concentration profile (acid soluble) and capillary water saturation. The chloride analysis was performed according to the following protocol. The concrete sample is finely ground and about 1 g of powder is dissolved in heated diluted nitric acid and the chlorides are quantified with an ion selective electrode. The cement content is measured by titration with ethylenediaminetetraacetic acid (EDTA) and photometric measurement of the color change with a murimex indicator. The capillary saturation (S) was evaluated based on the following equation:

$$S = \frac{m_{\text{sample}} - m_{\text{dry}}}{m_{\text{saturated}} - m_{\text{dry}}} \quad (1)$$

where m_{sample} is the weight of the original sample, m_{dry} is the sample weight after drying at 105 °C and $m_{\text{saturated}}$ is the weight after the capillary water saturation. The capillary saturation test was performed according to Ref. [7].

3 Results and discussion

3.1 Electrochemical experiments

The electrochemical experiment was performed to evaluate at which potentials the corrosion rate increased in concrete samples with 1 and 2% Cl^- by mass of cement. These potentials are then compared to the measured potentials in the cooling water tunnel to evaluate the risk of galvanic corrosion. The chloride concentration of the concrete in the cooling water tunnel is also compared to the chloride concentration used in the electrochemical experiment. Table 2 shows the mass loss as g/m^2 measured by repeated pickling of all exposed samples. The mass of the original oxide scale in the received samples was estimated to $136 \pm 9\ g/m^2$ as measured by repeated pickling of 10 unexposed samples of 13 cm lengths. Since this mass is included in the pickling results it is necessary to remove this offset before calculating the corrosion rate. A constant offset of $136\ g/m^2$ was used for all samples as it was not possible to determine the

Table 2. Mass loss measured by repeated pickling

% Cl by mass of cement	Potential (mV) (SCE)	Exposure days	Corrosion (g/m^2)
1	−100	88	330
1	−200	88	134
1	−300	83	142
1	−400	105	154
1	−500	105	150
1	−600	105	158
1	−700	66	150
1	−800	66	140
1	Unpolarized	238	137
2	−100	18	444
2	−200	19	319
2	−300	74	430
2	−400	102	157
2	−500	105	146
2	−600	105	139
2	−700	105	143
2	−800	105	132
2	Unpolarized	238	159

thickness on an individual sample basis after exposure. As can be seen in Table 2, the exposure periods of the samples varies, and the samples may have been affected by different time dependent corrosion processes.

For samples with 1% Cl^- by mass of cement, the average corrosion rate, calculated based on this procedure, was between −1 and 10 µm/year except for the sample polarized to −100 mV which had considerably higher corrosion rate, 100 µm/year. As a general value, corrosion is considered to be initiated when the current density is constantly higher than 0.1–0.2 $\mu A/cm^2$ [3] which corresponds to 1.2–2.3 µm/year, i.e. the rebar is considered passive if the corrosion rate is lower than about 2 µm/year. The corrosion rate for almost all samples polarized to different potentials, −800 to −100 mV, is higher than about 2 µm/year and is therefore not in a passive state. However, the corrosion rate, measured by pickling, has an uncertainty that can be estimated based on the standard deviation of the oxide scale weight. To investigate if the measured corrosion rate at each potential is statistically significant a confidence interval of 95% certainty (116–156 g/m^2) is compared to the measured corrosion values. Corrosion values within this interval may only be a result of variations of the oxide scale. The only mass loss which is outside this confidence interval is the sample polarized to −100 and −600 mV for samples with 1% Cl^- by mass of cement, however, the value for the sample polarized at −600 mV is very close to the upper interval boundary.

Small corrosion pits were seen on the surface after pickling the sample with 1% Cl^- by mass of weight polarized to −700, −600, −500, and −400 mV. As the measured current density during polarization was low for these samples (<0.2 $\mu A/cm^2$), the observed corrosion pits may have been formed during hardening. The risk of galvanic corrosion is here defined as when the mass loss increases rapidly from a certain potential, i.e. the potential where the steel surface changes from a passive state with a low corrosion rate to an active state (pitting) with high corrosion rate. Based on these observations, we conclude that steel in concrete with 1% Cl^- by mass of cement has a high risk of galvanic corrosion if polarized more anodically than −200 mV (SCE). The reason why −200 mV is chosen and not −100 mV is that there may be an initiation between −100 and −200 mV, which is not tested, therefore the highest potential without corrosion initiation is chosen.

Based on mass loss values in Table 2, samples with 2% Cl^- by mass of cement and polarized in the interval −500 and −800 mV had an average corrosion rate between −1.8 and 4.4 µm/year. However, these values are not significant considering variations in the oxide scale since the original mass loss values are within the 95% confidence interval as described above. In contrast, the values for samples polarized in the interval from −400 to −100 mV are all significant. The corrosion rate increased faster with more anodic potentials for samples polarized to −400 mV and higher. The corrosion rate at −400 mV is just outside the 95% confidence interval and the steel surface is therefore in an active state.

Figure 3 shows the current density during polarization for samples with 2% Cl^- by mass of cement. The sample with the highest polarization in anodic direction (−100 mV) also had the highest current density, followed by samples with smaller polarization, in decreasing order. Based on these experiments, we therefore conclude that the risk of galvanic corrosion for steel in concrete with 2% Cl^- by mass of cement is high when polarized above −500 mV (SCE). This potential is the highest anodic potential without active corrosion.

The corrosion rate for samples with 2% Cl^- by mass of cement as a function potential is seen in Fig. 4, where the corrosion rate is calculated by both taking the oxide scale into account and by not doing so. The curves in Fig. 4 are based on data in Table 2 or from the average current density measured during polarization taken from Fig. 3. The average corrosion rate measured during polarization and pickling is relatively similar for potentials more anodic than −400 mV and the calculated corrosion rate with subtracted scale is lower. It is possible that the oxide scale, which consists of mainly magnetite [8], is not stable at these potentials and chloride levels so that oxidation of both the scale and the bulk material may contribute to the current measured during polarization. A phase conversion of the oxide layer is also possible according to Equation (2) [9] when the sample is polarized in anodic direction:

$$3Fe_3O_4 \rightarrow 4\gamma - Fe_2O_3 + Fe^{2+} + 2e^- \quad (2)$$

The potential dependent current $i(E)$ may be divided into two parts according to Equation (3):

$$i(E) = i_c + i_F \quad (3)$$

where i_c is the corrosion current of the bulk material, i_F is the current of film growth/dissolution [10] and possibly conversion. It is possible that the total current, $i(E)$, corresponds to the average current during polarization and i_c corresponds to the current correlating to the mass loss measured by pickling without the oxide scale. In other words, the current that can be calculated by Faraday's law.

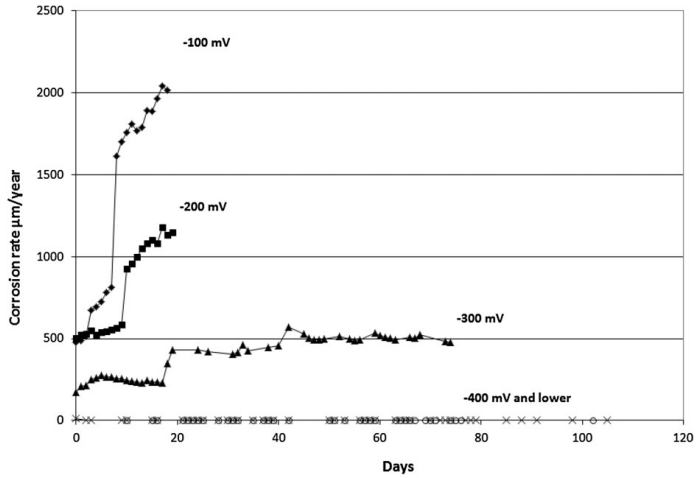

Figure 3. Corrosion rate *versus* time for samples with 2% chlorides by mass of cement. 100 µA/cm² corresponds to 1200 µm/year

The anodic current increased much faster at lower potentials for steel in concrete with 2% Cl^- than steel in concrete with 1% Cl^-. This is explained by the Pourbaix diagram in Fig. 5 where chlorides cause pitting and the highest pitting potential is lowered. With higher chloride concentration, the passive area will be even smaller.

It may also be interesting to assess the corrosion rate as an accepted reduction of the rebar diameter in such a way that the criteria of the mechanical properties of the rebar are still fulfilled. This means that it may be tolerable that the stainless steel pumps polarize the rebar to more anodic potentials than the indicated risk potentials measured in the electrochemical experiment. The concrete cover may crack when the radius reduction of the rebar is about 25–50 µm [11] for reinforced concrete exposed to atmospheric wet/dry cycles. However, in water saturated (or near saturated) concrete, corrosion products are more easily transported through the concrete cover to the surrounding seawater without causing concrete cover cracking. Therefore, a higher corrosion rate can be tolerated in water-saturated concrete than in atmospheric conditions. In the hypothetical case where the rebar diameter is 12 mm and, e.g. 10% reduction of the rebar diameter is accepted this means that a 1200 µm reduction is accepted during the structure's residual service life. If the

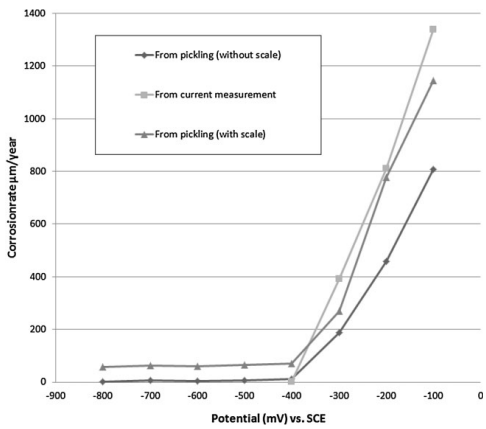

Figure 4. Corrosion rate for samples with 2% chlorides by mass of cement. Corrosion rate is measured by repeated pickling calculated with and without the oxide scale and calculated from the average corrosion current during polarization

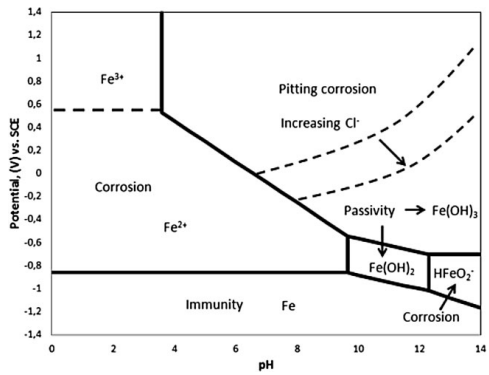

Figure 5. Pourbaix diagram of iron in water at 298 K and ion conc. 10^{-6} mol/L. The diagram is made for the most common formed iron hydroxides

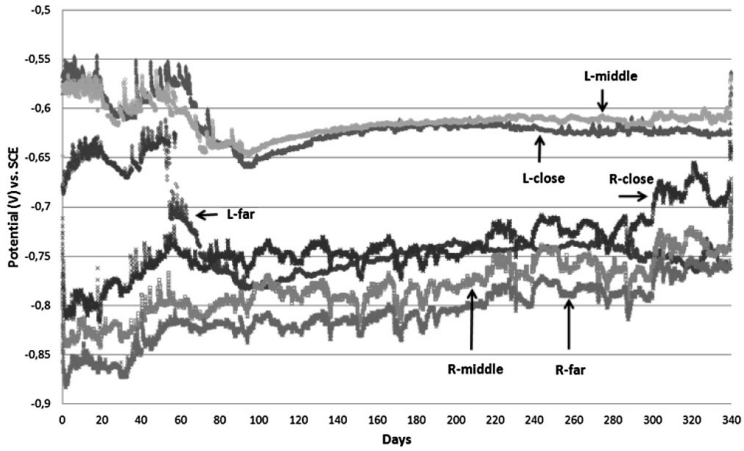

Figure 6. Measured potential over time at different sites in the cooling water tunnel. The left tunnel was without sacrifical anodes (L-close, L-middle, L-far) and the right tunnel was with sacrifical anodes (R-close, R-middle, R-far)

structures service life is stated to be 100 years, the accepted annual corrosion rate is 12 µm/year. If this corrosion rate is used as an accepted threshold corrosion rate, the high risk potential where the galvanic current increases rapidly is set to be −100 mV (SCE) for samples with 1% Cl^- by mass of cement and −300 mV for samples with 2% Cl^- by mass of cement.

The mortar sample made for the electrochemical study is young and is therefore not totally comparable with the concrete in the cooling water tunnel, which is 30 year old. Young concrete has usually higher pH of the pore solution compared to old concrete due to very low leaching of alkali [12]. On the other hand, old concrete in water is usually denser than young concrete due to longer hardening time [13].

3.2 Field study

The corrosion potential data from steel in concrete in the cooling water tunnels is shown in Fig. 6. At day zero, the cooling water tunnel was filled with water and the measurement of corrosion potential started. After about 340 days, the cooling water tunnels were emptied from water and the measurement stopped. The potentials measured in the left tunnel generally have more anodic potentials than the potentials in the right tunnel. The sacrificial anodes in the right tunnel, but not in the left, lower the potential to between −700 and −800 mV.

Reinforced concrete structures are regarded as protected by sacrificial anodes made of aluminum if the potential is lowered to −800 mV *versus* SCE [14]. The corrosion potentials in the right tunnel are more anodic close to the stainless steel pumps than further away. It is therefore likely that the stainless steel pumps polarize the reinforcement in anodic direction. As stated above, the more noble potentials in the left tunnel are mainly due to the absence of sacrificial anodes.

The pumps started after 20 days and after that the potentials in the right tunnel increased until about 60 days. It is likely that the measured potentials are affected by the water flow and the water temperature. If the water flow is low then is also the transport of oxygen to the stainless steel surface low leading to concentration polarization. This would mean that the sacrificial anodes are consumed at a low rate and the risk of galvanic corrosion would also be low. When the water flow increases, the transportation of oxygen to the stainless steel surface increases, leading to an increased cathodic current and higher consumption rate of the sacrificial anodes. This is explained by Fig. 7, which

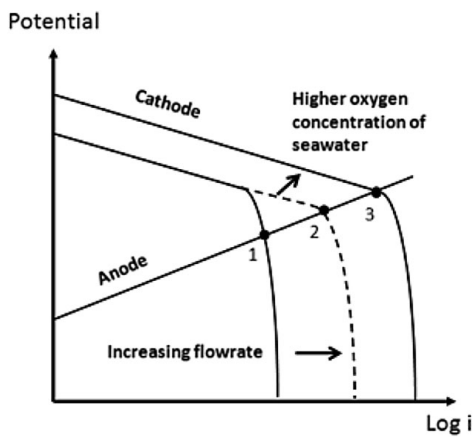

Figure 7. Schematic figure of the potential–current relationship between the anodic reaction of the sacrificial anode and the oxygen reduction reaction on the stainless steel surface affected by the flow rate and oxygen concentration of sea water [15]. The effect of seawater resistivity is not regarded

shows a schematic picture of the potential–current relation where the anode is the sacrificial anode and the cathode is the rebars and pumps. Point 1 is the protective current from the sacrificial anode during the first 20 days where the flow rate is low. When the flow rate increases both the anodic current of the sacrificial anode and the potential of the stainless steel pumps increase to point 2. This equilibrium was probably established from 20 days to 60 days. The anodic current from the anode is relatively high and even reaches the rebars furthest away from the pumps in the left tunnel. This is shown as a potential drop for "L-far" after 55 days. It cannot be excluded that the reinforcement in the left tunnel closer to the pump also has some cathodic protection after 60 days, measured by "L-middle" and "L-close".

The water temperature affects corrosion in several ways by changing the resistivity of seawater and the oxygen concentration of the seawater. Therefore, it is important to assess how the water temperature affect the risk of galvanic corrosion in the cooling water tunnel as well as the consumption rate of the sacrificial anodes. With lower water temperature, both the resistivity of water and the solubility of oxygen increase. This has two different effects. If the water temperature is lowered, the sacrificial anode will be less able to protect the rebar and stainless steel pumps due to higher resistivity. Subsequently, the consumption rate of the anodes would be lower and the potential difference between the anodes and the stainless steel would increase. On the other hand, higher solubility of oxygen in seawater would increase the rate of the oxygen reduction reaction on the stainless steel surface leading to more anodic potentials and higher consumption rate of the anodes, see point 3 in Fig. 7.

The temperature of the cooling water is given in Fig. 8 and varied between 0 and 23 °C. The annual average water temperature was 10 °C. The temperature was lowered from about 20 °C at 60 days to about 0 °C at 180 days and the anodic current should then have increased and the potential should have risen to point 3 in Fig. 7. However, such changes were not seen as the potential was relatively stable during that time period. Because the water temperature has the two discussed mechanisms makes it very difficult to assess the risk of galvanic corrosion and the consumption rate of the anodes by only assessing the water temperature. The measured potentials were stable during temperature variations, this conclude that the high consumption rate of the sacrificial anodes is probably not an effect by temperature.

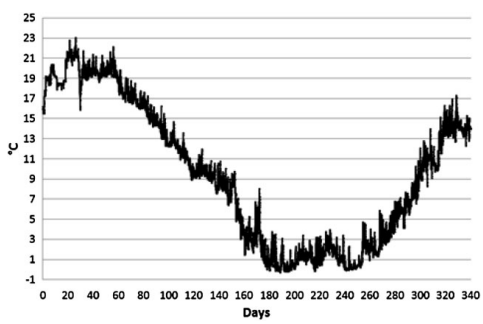

Figure 8. Measured temperature of seawater in the tunnel

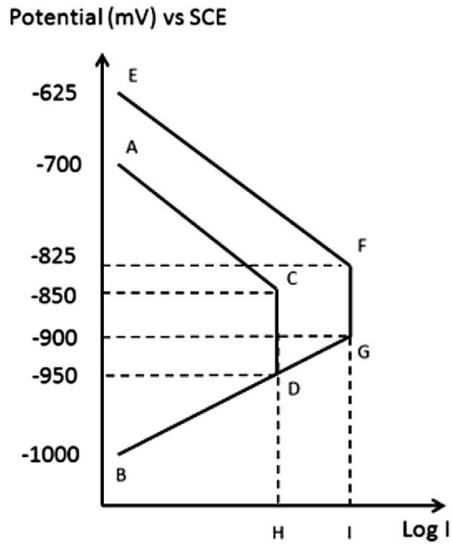

Figure 9. Schematic potential–current diagram when sacrificial anode is connected to the steel rebar and when it is connected to both the stainless steel pumps and the steel rebar. The resistivity of the concrete causes an IR-drop (discussed in the text)

The high consumption rate of the sacrificial anodes is most likely explained by Fig. 9 which shows a schematic potential–current diagram for the two cases when only the rebar is connected to sacrificial anodes and when both the rebar and stainless steel pump is connected to the sacrificial anodes. Point A is the potential of steel in water-saturated concrete, which is about −700 mV. Point B is the potential of the Al–Zn–In sacrificial anode, which is about −1000 mV in seawater [14]. When the rebar and the sacrificial anode are connected, the rebar is a cathode and the sacrificial anode is an anode. When they are in contact the rebar potential is lowered to point C and the anode potential is raised to point D, about −950 mV. There is thus a potential difference between point C and D because of the resistance of the concrete; this is usually called an IR drop [16]. The sacrificial anode is then consumed with the corrosion rate of H.

Point E is the potential of about −620 mV for the mixed potential of the rebars and the stainless steel pumps in seawater. When the rebar and stainless steel is connected to the sacrificial anode this potential is lowered to about −825 mV (point F) and the potential of the anode is raised to point G. The current of the sacrificial anode is then raised to point I. The sacrificial anodes are consumed much faster at point I as the current increases logarithmically with potential. This explains mostly why the sacrificial anodes were consumed more rapidly than expected in the cooling water tunnel. Although, high flow rate also seems to increase the consumption of the sacrificial anodes and the temperature variations seem to have a minor effect.

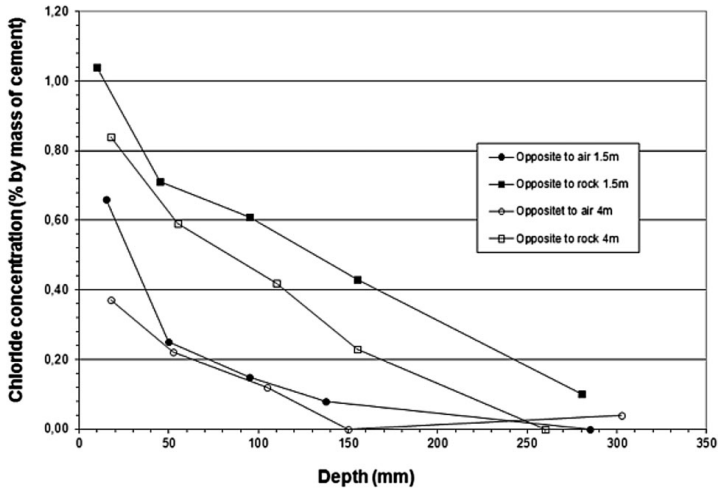

Figure 10. Chloride concentration profiles of the drill core samples taken from the left side (opposite to air) and right side (opposite to rock) of the right channel, as marked in Fig. 6

Chloride analyses of the concrete drill core samples are shown in Fig. 10. The chloride content is higher for the concrete with rock on the opposite side than the concrete with air on the opposite side. At a concrete cover of about 50 mm the chloride content is about 0.3 and 0.7% Cl^- by mass off cement for concrete opposite to air and rock, respectively. If a wall made of concrete with high permeability for water flow is exposed to water on one side and air on the other side, water will be capillary transported within the wall. At a certain distance, the water evaporates and chlorides accumulate [17]. An accumulation of chloride would increase the corrosion rate, which is supported by the higher corrosion rate with 2% Cl^- by mass of cement compared to 1% Cl^- by mass of cement in the electrochemical study. The concrete in the cooling water tunnels has a w/c about 0.6, which is a relatively permeable concrete. However, it cannot be seen that the chloride concentration is higher at any depth due to chlorides have been accumulated. The capillary saturation of concrete opposite to rock is higher than that of concrete opposite to air. For concrete opposite to rock, the capillary saturation was about 95% and for concrete opposite to air the capillary saturation was about 85%. It is reasonable that the concrete wall opposite to air has a lower capillary saturation due to drying on the air side.

The experimental study showed that rebar with 1% Cl^- had to be polarized to about −200 mV for an increased risk of galvanic corrosion. The measured chloride concentration for the drill core samples were all under 1% Cl^- and the measured potential in the cooling water tunnel was never as high as −500 mV. Therefore, it is not likely that the rebar suffer of galvanic corrosion according to the measured potentials. However, the potential of the steel reinforcement in the absolute vicinity to the stainless steel pumps may not have been measured very well due to long distance between the potential logger and pumps. Therefore, the steel reinforcement close to the pumps may suffer of galvanic corrosion.

4 Conclusions

The measured potentials in the cooling water tunnels did not reach more positive potentials than about −600 mV (SCE) on the side in the tunnel without sacrificial anodes and the potential was lowered to between −700 and −800 mV on the side with anodes. The cathodic protection was improved with distance from the stainless steel pumps.

The highest measured chloride concentration in the cooling water tunnels was 0.7 by mass of cement. The electrochemical experiment showed that the risk of galvanic corrosion for steel in concrete with 1% Cl^- by mass of cement is raised when the potential is anodically polarized to above −200 mV (*vs.* SCE). For concrete with 2% Cl^- by mass of cement, the risk of galvanic corrosion increases at potentials more anodic than −500 mV. These results support that the rebar in the cooling water tunnel does not suffer of galvanic corrosion.

The unexpected rapid consumption of the sacrificial anodes is mainly explained by the unintentional connection between the rebar in concrete and the stainless steel pumps. The stainless steel pumps have a relatively noble potential and together with a high flow rate this will lead to an increased anodic current from the sacrificial anodes.

The steel reinforcement closer to the stainless steel pumps has a higher risk of galvanic corrosion compared to the steel bars situated at longer distances from the pumps.

Potential data loggers are suitable for corrosion monitoring of structures with water saturated concrete.

Acknowledgements: This research was funded by Elforsk and SBUF, which is gratefully acknowledged by the authors. The authors would also like to acknowledge *Mikael Oxfall*, Vattenfall Research, and development, for his work with the capillary saturation tests and Mr. *Bror Sederholm*, Swerea KIMAB, for fruitful discussions and critical comments on the manuscript.

5 References

[1] C. Abreu, M. Cristóbal, M. Montemor, *Electrochim. Acta* **2002**, *47*, 2271.
[2] S. Qian, D. Qu, *J. Appl. Electrochem.* **2010**, *40*, 247.
[3] U. Angst, B. Elsener, C. K. Larsen, Ø. Vennesland, *Cement. Concrete. Res.* **2009**, *39*, 1122.
[4] P. Sandberg, *Ph. D. Thesis*, Lund University, Lund, **1998**.
[5] L. Li, A. A. Sagues, *Corrosion* **2001**, *57*, 19.
[6] W. von Baeckmann, *Handbook of Cathodic Corrosion Protection*, Gulf Publishing Company, Houston **1997**.
[7] G. Hedenblad, L.-O. Nilsson, *Degree of Capillary Saturation*, Division of Building Materials, Lund University, Lund, Report TVBM-7005, **1985**.
[8] P. Ghods, O. Isgor, G. McRae, *Corros. Sci.* **2011**, *53*, 946.
[9] C. Alonso, C. Andrade, X. Novoa, *Corros. Sci.* **1998**, *40*, 1379.
[10] Z.-T. Chang, B. Cherry, M. Marosszeky, *Corros. Sci.* **2008**, *50*, 3078.
[11] H. Wong, Y. Zhao, A. Karimi, *Corros. Sci.* **2010**, *52*, 2469.
[12] D. Jacques, L. Wang, E. Martens, *Cement. Concrete. Res.* **2010**, *40*, 1306.
[13] L. Bertolini, Luca. B. Elsener, P. Pedeferri, *Corrosion of Steel in Concrete. Prevention, Diagnosis, Repair*, Wiley VCH, Weinheim **2004**.
[14] *Cathodic Protection Design*, Recommended Practice. Det Norske Veritas, DNV-RP-B401, **2010**.
[15] G. Wranglen, *Metallers Korrosion Och Ytskydd*, (in Swedish), Almqvist & Wiksell Förlag, Stockholm **1967**.
[16] D. Jones, *Principles and Prevention of Corrosion*, Prentice Hall, Englewood Cliffs, NJ **1996**.
[17] S. Lindmark, B. Sederholm, *Korrosion På stål i Betong i Kylvattenvägar-Delrapport 1, Litteraturgranskning*. (in Swedish) Elforsk Rapport 10:82, **2010**.

(Received: April 3, 2013) W7141
(Accepted: July 1, 2013)

Paper II

Influence of chloride and moisture content on steel rebar corrosion in concrete

J. Ahlström, J. Tidblad, B. Sederholm and L. Wadsö

Abstract

The objective of this study was to investigate corrosion of steel in mortar at various chloride and moisture levels. The samples were exposed in humidity chambers with different relative humidity or exposed in cyclic moisture conditions. The lowest chloride concentration that initiated corrosion was 1% Cl by mass of cement, corrosion was then seen for samples exposed at 97% relative humidity. It is suggested that the corrosion rate decreases when samples are exposed to a relative humidity lower than 97%. For samples exposed to cyclic moisture conditions, a lower chloride concentration was needed to initiate corrosion compared to samples exposed in static moisture conditions.

1.0 Introduction

Chloride induced corrosion of reinforcement steel is a frequently observed corrosion mechanism in concrete structures [1]. The structures are exposed to chloride ions from the surrounding environment and these are transported through the concrete to the steel surface. There, a chloride containing local environment is formed at the steel surface that increases the solubility of corrosion products. This results in a significant increase in the corrosion rate. In an uncontaminated concrete, without chlorides, iron-oxides/oxyhydroxide/hydroxides are formed on the steel surface and these have low solubility due to the high pH of the pore water solution.

Many attempts have been performed to determine the critical chloride threshold level (CTL) in concrete, the chloride concentration at which the corrosion rate increases. A review of reported CTLs measured in the laboratory can be found in reference [2]. Experimentally measured CTLs range from close to zero to about 2.5 mass-% Cl (by mass of binder). A review of reported chloride concentrations in exposed structures with observed corrosion damage can be found in reference [3]. The reported chloride concentrations from these structures also ranged from close to zero to about 2.5 mass-% Cl (by mass of cement). The relatively large range of reported critical CTLs may be explained by the use of various experimental setups and the fact that corrosion is affected by several factors, e.g. moisture condition, type of concrete, type of steel, and temperature.

The electrochemical reactions, the anodic reaction and cathodic reaction, describing corrosion of steel in concrete are

$$2Fe \rightarrow 2Fe^{2+} + 4e^{-}$$

$$2H_2O + O_2 + 4e^{-} \rightarrow 4OH^{-}$$

The anodic reaction is oxidation of iron which produces electrons. The cathodic reaction is reduction of oxygen which consumes the electrons.

The transport rate of oxygen to the steel surface is the main controlling factor for the corrosion rate, and this transport rate is mainly determined by the water/cement-ratio of the concrete and the moisture conditions in the concrete. One of the first studies to assess how the moisture conditions affect the corrosion rate was performed by Tuutti in 1982 [4]. In his study reinforced concrete samples had either been carbonated or were prepared with $CaCl_2$ in the mixing water. The oxide scale on the steel

surface that is formed at manufacturing was removed before casting. The study showed that the corrosion rate had a strong relation to the moisture condition and that the highest corrosion rate was measured for samples exposed to about 90-95% relative humidity.

Chlorides are hygroscopic [5], meaning that chlorides by themselves are affecting the moisture condition in the concrete. The present study was performed to assess how different specific chloride concentrations affect the moisture conditions in concrete and thereby the corrosion rate. The corrosion rate was measured with repeated pickling, a simple test method without the experimental difficulties related to electrochemical methods. Mortar samples were cast with steel bars without removing the oxide scale formed at manufacturing.

2. Materials and methods

The corrosion rate of steel in mortar was assessed by exposing samples consisting of cylindrical steel bars cast in mortar contaminated with chloride at different levels and exposed to atmospheres with different relative humidity (RH) levels. When the mortar was in equilibrium with the humid air, after 3 months, samples were cracked and the steel bars evaluated for mass loss. This was repeated after an additional 12 months for samples.

2.1 Sample preparation

The composition of the carbon steel used (S235JR according to EN 10025-2:2004) is shown in Table 1.

Table 1
Chemical composition of the steel bars (% mass).

C	Mn	P	S	N	Cu
0.17	1.4	0.035	0.035	0.12	0.55

A schematic drawing of a mortar sample with the steel rebar can be seen in Fig. 1. The steel bars had a diameter of 12 mm and were cut into 130 mm long cylinders. The surface of the steel bars was smooth and in an as-received condition with the oxide scale intact. Before casting, the steel bars were degreased with trichlorethylene. The degreasing procedure was 30 seconds in steam followed by 5 minutes in an ultrasound bath. This procedure was repeated 4 times. To minimize the risk of having existing active areas on the steel surfaces before casting, the steel bars were immersed into a synthetic pore water solution for 48 hours. The synthetic pore water solution was mixed with the following molar ratios: 0.1 NaOH, 0.3 KOH, 0.03, $Ca(OH)_2$ and 0.02 $CaSO_4 \cdot H_2O$.

As a final step before casting, one end of the steel bars was covered with a varnish, (Lacomit , Agar Scientific Ltd. UK) and inserted into a plastic ring with a thickness of 5 mm, which was then inserted into a plastic tube. Finally, the mortar was poured into the plastic tube and placed on a vibration table for 30 seconds. In this way a mortar cover of about 5 mm was obtained around the steel bar. The mortar was made by mixing a Portland cement (CEM I 42.5 N - SR 3 MH/LA ‘Anläggningscement Degerhamn’, Cementa AB, Sweden) and sand (DIN EN 196-1, ‘Normensand’) with a maximum particle size of 2 mm. The mortar was mixed with water/cement/sand mass proportions of 1/2/3 corresponding to a water cement ratio of 0.5. To avoid large air voids, a water reducing agent (Sikament EVO 26) and an air reducer (Sika PerFin-300) was added to the mixing water. Finally, the mortar samples were cured for 30 days with the plastic tubes stored in plastic bags together with wet towels. The plastic bags with samples were weighed before and after curing to ensure that the bags were not leaking.

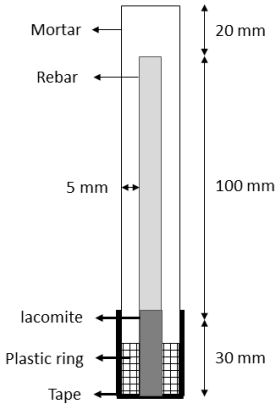

Fig. 1. Schematic figure of the mortar samples with steel rebar.

In addition to the sample configuration indicated in Fig. 1 a few additional samples was made where one side of the sample surface was covered with butyl tape. This was done to assess the corrosion rate when one side has a decreased transportat of oxygen. In this way it may be possible that a macrocell is formed.

Two different methods were used to introduce chlorides into the mortar, either by adding NaCl to the mixing water or by capillary suction. For the mixing water method, a series of mortar samples was prepared with Cl^- concentrations of 0, 0.2%, 0.4%, 0.6%, 1.0%, 1.5% and 2.0 weight-% Cl^- by mass of cement. The concentration "weight-% Cl^- by mass of cement" will hereafter be referred to as "% Cl". For the capillary suction method, only two levels of Cl^- were prepared. After hardening, the mortar samples were first conditioned in a vacuum chamber for approximately 3 weeks. Thereafter, the samples were inserted into NaCl solutions with either 0.08 or 0.12 mol Cl^- L^{-1}. Immediately after insertion, bubbles were seen on the surface and when no new bubbles were formed, the samples were taken out. The salt bath exposure took about 3 days. After the salt bath exposure the samples were dried with a paper towel and placed in the specific relative humidity chambers.

2.1.1. Exposure conditions

Levels of constant RH were obtained by placing saturated salt solutions in desiccators. The samples were standing on perforated ceramic plates placed above a salt solution. A fan was mounted under the ceramic plate blowing on the salt solution to minimize gradients and establish a stable moisture condition throughout the entire desiccator by facilitating exchange of air between the compartments below and above the ceramic plate. The different saturated salt solutions and corresponding RH levels are given in Table 2. The samples' moisture content was controlled by weighing three samples for each exposure condition at regular intervals throughout the exposure period. The measured masses after hardening were used as reference masses.

Table 2
Saturated salt solutions and corresponding relative humidity (RH) values.

Saturated salt solution	RH
NaCl	75%
KCl	85%
$BaCl_2$	91%
KNO_3	94%
K_2SO_4	97%
H_2O	100%

A few samples were exposed to cyclic moisture conditions. This was achieved by alternating the samples between desiccators containing 100% RH and 75% RH every 30 days.

2.1.2 Corrosion measurements

The average corrosion rate after different exposure times was measured by repeated pickling (ISO 8407) in Clark's solution: 20 g Sb_2O_3 and 60 g $SnCl_2$ per liter HCl 37%. As the steel was exposed in an as-received condition, the oxide scale present already before exposure is also removed from the steel surface during pickling and contributes to the total measured mass loss. Therefore, unexposed samples were also pickled to quantify the average mass and thickness of the oxide scale. In order to report a correct corrosion rate it is necessary to subtract the mass loss from the preexisting oxide scale from the total weight loss of exposed samples. This procedure of taking into account the effect of the oxide scale is new and is described in more detail in reference [6].

2.1.3 Measurement of mortar properties

The moisture content by mass of dry mortar (u) was evaluated based on equation 1 and the capillary saturation (S) was evaluated based equation 2:

$$u = \frac{m_{sample} - m_{dry}}{m_{dry}} \qquad \text{Eq 1}$$

$$S = \frac{m_{sample} - m_{dry}}{m_{saturated} - m_{dry}} \qquad \text{Eq 2}$$

where m_{sample} is the mass of the evaluated sample, m_{dry} is the mass after drying the sample at 105 °C and $m_{\text{saturated}}$ is the mass after the capillary water saturation. The capillary saturation was performed according to reference [7].

The water activity was measured on crushed material in a glass test tube with a relative humidity probe (HOBO Pro V2, Onset). The probes were calibrated by measuring the relative humidity over saturated salt solutions in test tubes.

For the chloride analysis, mortar samples were finely ground and about 1 g of powder was dissolved in heated diluted nitric acid (7%). The chloride concentration of the solution was then quantified with an ion-selective electrode. The CaO content was measured by titration of the same solution with ethylenediaminetetraacetic acid (EDTA) and photometric measurement of the color change with a murimex indicator. The cement content was obtained by assuming that the cement contained 63% CaO.

3. Results and discussion

3.1 Assessment of moisture condition

Fig. 2. Weight change vs exposure time of samples with 0.4% Cl exposed at different RH from 75% to 100%.

Measurements of weight change were performed to check whether the samples increased or decreased in weight. Figure 2 shows the weight change of samples with 0.4% Cl exposed at different RH. Most of the weight change was observed during the first 100 days. The relatively small weight changes after 100 days indicate that moisture conditions were stable in the mortar samples exposed to 75 – 94% RH.

Samples exposed in 75, 85, 91, and 94% RH decreased in weight (dried) whereas samples exposed in 97 and 100% RH increased in weight (gained water). The weight changes for the latter samples were fluctuating to a higher degree compared to samples with lower relative humidity, which is not surprising since it is difficult to avoid water condensation in desiccators at high RH levels.

The samples' mass change is not only affected by the moisture condition in the mortar. If carbonation occurs, the weight of the formed calcium carbonate would increase the weight of the samples. Corrosion of the steel in mortar would also increase the mass of the samples. However, any mass change due to the two mentioned mechanisms was not detectable except for samples with 2% Cl by mass of cement. Samples with 2% Cl by mass of cement did increase in weight (0.5-3 g) due to corrosion products (indicated by cracks in the mortar cover). To conclude, and as indicated by the stable conditions reached after 100 days (see Fig. 2), the activity of water in the different experiments match the relative humidity levels of the respective exposure environments.

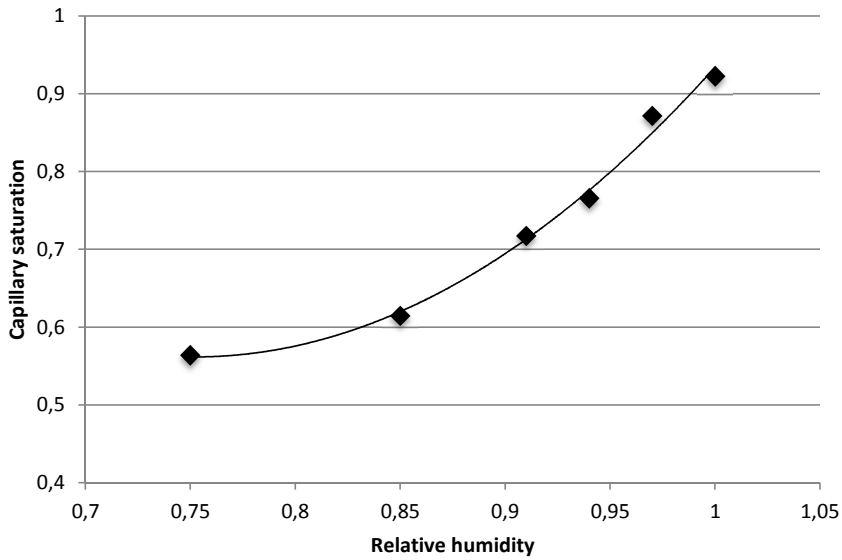

Fig. 3. Capillary saturation vs. RH of samples with 0.4 % Cl after 15 days of exposure

To understand the moisture conditions in the mortars it is necessary to measure both the RH and the capillary saturation (Eq. 2). When the RH is below 45%, water is adsorbed on the pore walls. At higher RH, water also starts to condense between narrow pore surfaces (capillary condensation). How much condensate that is formed cannot be determined only by the RH since the amount of condensate

is also determined by the pore structure and the composition of the pore water. Another measure of the amount of moisture is therefore needed, and we have chosen to also measure the capillary saturation as a function of RH, i.e. the ratio between the mass of water in a sample and the mass of water that the sample will take up by capillary suction. The capillary saturation is a measure of how much liquid water that is in the pore system, and thus also a measure of how much water that can act as an electrolyte for corrosion processes.

The capillary saturation was measured for all samples, i.e. as a function of the chloride concentration and RH. Fig. 3 shows results for a constant level of chloride contamination. The capillary saturation increases with RH as expected. For a sample with 0.4% Cl by mass of cement the capillary saturation was about 0.55 in 75% RH and about 0.9 in 100% RH. The capillary saturation did not reach 1.0 at 100% RH. A much longer time than used in this experiment will be needed for the pores to be filled with water.

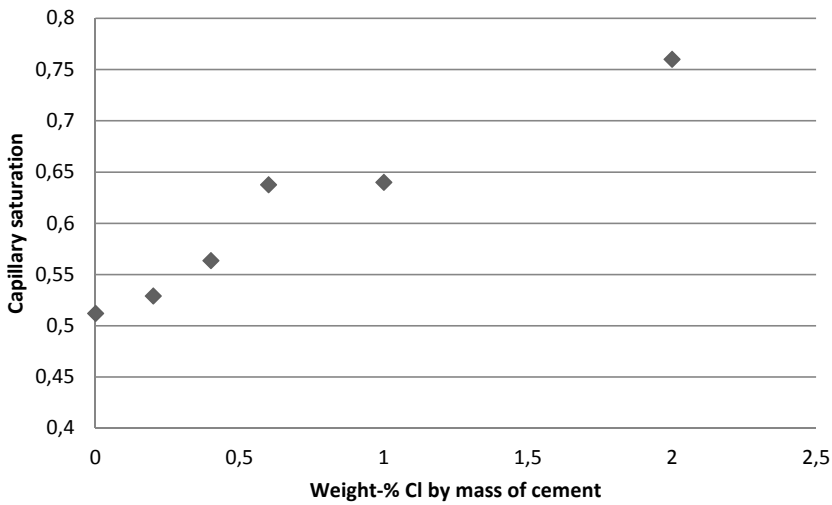

Fig. 4. The capillary saturation of samples with various chloride concentrations exposed in 75% RH.

The pore water composition also affects the capillary saturation, in our case depending on the chloride concentration. Increasing the concentration of chloride in the mortar also increases the free chloride level in the pore solution [8], which means that the capillary saturation increases in a sample with chlorides compared to a sample without chlorides. With chlorides, more water is adsorbed onto the pore walls and this narrows the air gap in the pore and condensates are more easily formed. This is illustrated in Fig. 4, which shows the capillary saturation of samples with different chloride concentrations exposed at 75% RH. The capillary saturation was about 0.5 for a sample without chloride and about 0.75 for a sample with 2% Cl by mass of cement. Generally, samples with no chlorides had the lowest capillary saturation and the capillary saturation increased with increasing chloride concentration. However, the difference in capillary saturation between samples with different chloride concentration was smaller for samples exposed at higher RH.

3.2 Assessment of chloride concentration

During casting, chlorides were added with the mixing water to obtain various chloride concentrations in the samples, in terms of % Cl. Chloride levels were measured on eight cast samples to check whether the target chloride concentrations, calculated from the mixing ratio, were obtained (Table 3). For samples with calculated chloride concentrations up to 1%, the measured and calculated concentrations are in fairly good agreement. For samples with 1.5% and 2.0% (calculated) chloride concentration exposed in 97% RH, the measured concentrations are lower than the corresponding calculated concentrations. For samples with 1.5% chloride concentration exposed in 91% RH, the calculated and measured concentrations are similar. This was also the case for samples with 2% chloride concentration exposed in 75% RH.

Table 3
Samples' chloride concentration, given as weight-% Cl by mass of cement.

RH exposure	Calculated concentration based on mixing ratio [%]	Measured concentration [%]
97%	0.2	0.2
100%	0.4	0.3
97%	0.6	0.6
97%	1.0	0.9
97%	1.5	1.1
91%	1.5	1.4
97%	2.0	1.3
75%	2.0	1.8

The lower measured chloride concentration compared to the calculated concentration for samples with 1.5 and 2.0% chloride concentration exposed in 97% RH can be explained by chlorides leaching out from the pore water solution forming salt crystals at the samples surface. This is consistent with the observation that the differences between calculated and measured concentrations are small at low RH. Visual observation confirmed the occurrence of salt crystals forming on the samples surface at high RH and high chloride concentrations. It is also possible that chloride containing droplets forming at the surface due to condensation falls off in an uncontrolled manner. In the following discussion of corrosion rates, given values of chloride concentration are the nominal calculated concentrations based on the mixing ratio, not the measured concentrations.

Chlorides were also introduced by capillary suction by immersion of the samples into 0.08M or 0.12M Cl solution. The measured chloride concentrations in the samples were 0.2% Cl and 0.3% Cl, respectively.

3.3 Assessment of corrosion rate for samples exposed in stationary conditions

As discussed before in connection with Fig. 2, it took about three months for the samples to obtain a stable moisture level. Figure 5 shows values of corrosion rate at various RH and chloride levels for samples evaluated shortly after this time. It should be noted that the corrosion values given in Fig. 5 are corrected for the occurrence of a preexisting oxide scale, described in more detail in reference [6]. The thickness of the oxide scale varies from sample to sample since the scale is unevenly distributed at the steel surface but the correction is made using a single value of 136±9 g/m^2, which explains the occurrence of negative numbers in Fig. 5 within the uncertainty level of the scale thickness. Samples with chloride concentrations from 0.2 to 1.0% Cl had a corrosion rate below the detection limit.

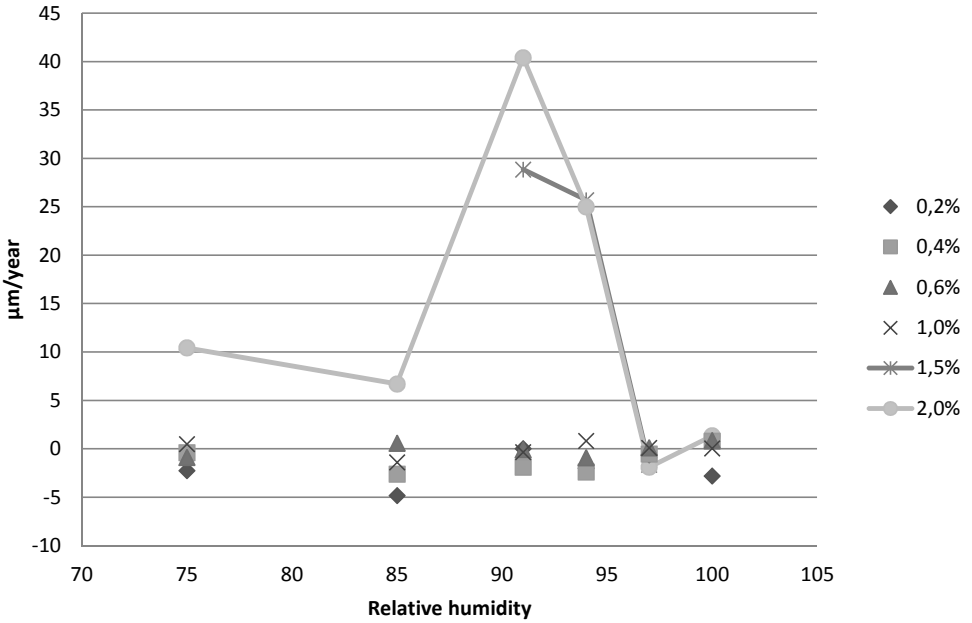

Fig. 5. Corrosion rate vs. RH after three months of exposure at different chloride concentrations (weight% Cl by mass of cement). The corrosion rate was calculated after subtraction of the preexisting oxide scale.

For samples with 2.0% Cl, the corrosion rate was about 10 and 7 µm/year exposed in 75% and 85% RH, respectively. The corrosion rate was considerably higher in 91 and 94% RH for samples with 1.5 and 2.0 % Cl. This was also confirmed by visual observation of early formed cracks in the mortar cover of these samples. The highest corrosion rate for samples with 2.0 % Cl was about 40 µm/year exposed in 91% RH and second highest was 25 µm/year exposed in 94% RH. The corrosion rate was below the detection limit in 97% and 100% RH. The capillary saturation was 1.0 (completely saturated) at 97% and 100% RH for 2.0 % Cl, which decreases the oxygen transport significantly.

To summarize, samples with chloride concentrations from 0.2 to 1.0% Cl had negligible corrosion rates. The corrosion rate for samples with 2.0% Cl had a clear dependence of moisture condition, where the highest corrosion rate was measured at 91% and 94% RH. The lower corrosion rates at 75% and 85% RH can be explained by higher resistivity of the mortar cover due to the low water content. The lower corrosion rates at 97% and 100% RH may be explained by slow transport of oxygen to the steel surface due to the high water content.

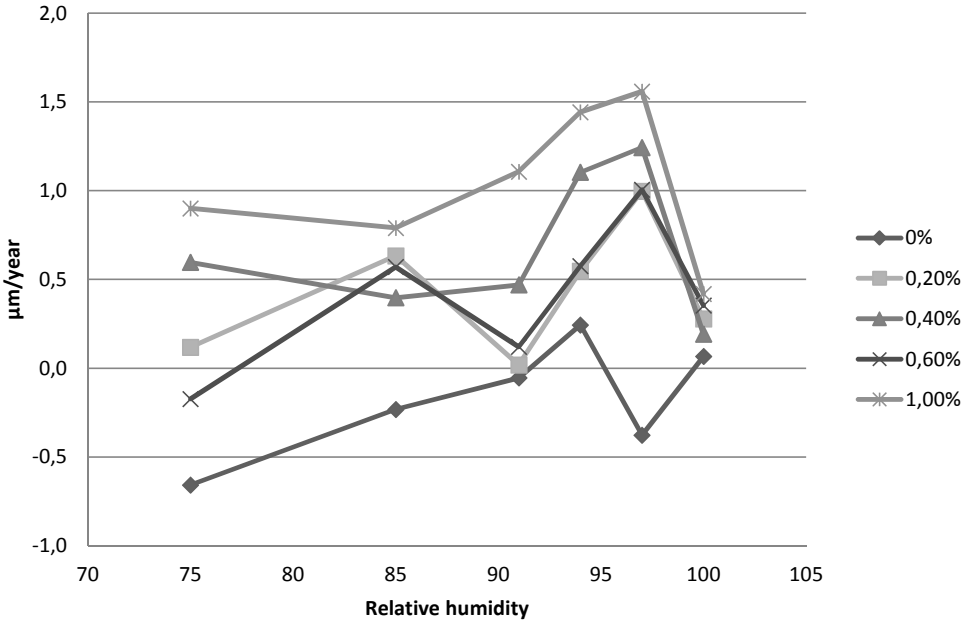

Fig. 6. Corrosion rate vs. RH after approximetly 15 months of exposure at differentchloride concentrations (weight% Cl by mass of cement). The corrosion rate was calculated after subtraction of the preexisting oxide scale.

The corrosion rate was also measured on a second set of samples about one year later (Fig. 6). Unfortunately, it was not possible to prolong the exposure period for samples with 1.5 and 2% Cl by mass of cement exposed to 91% and 94% RH, i.e. for those samples with highest corrosion rates after the first exposure period (Fig. 5). This was due to cracks in the mortar cover. The average corrosion rate of all samples without chlorides was below the detection limit, which corresponds to passivity. The corrosion rates of samples with chloride concentration from 0.2 to 1.0 % Cl were also relatively low and the average corrosion rate was 0.6 µm/year, which is still below the uncertainty of the oxide scale thickness corresponding to ±0.9 µm/year for this exposure period. Samples with 1% Cl had the highest corrosion rate of about 1.6 µm/year exposed in 97% RH. This corrosion rate was high enough to cause small cracks in the 5 mm mortar cover of one of three samples. This suggests that the chloride concentration is high enough to form a relatively large active area on the steel. In Fig 6, there is a tendency indicating a corrosion rate dependence of moisture condition with a maximum at 97% RH based on values for all samples with chloride concentration ranging from 0.2 to 1.0% Cl. Table 4 shows a summary of corrosion rates for exposures at different RH and chloride levels. For simplification all exposures with chloride levels between 0.2% and 1.0% have been grouped together.

Table 4
Summary of corrosion rates for exposures at different RH and chloride levels (n.s. = not significant).

RH %	Cl = 2% t = 3 months	Cl = 2% t = 15 months	0.2% < Cl < 1% t = 15 months
75	10	1.8	n.s.
85	7	19	n.s.
91	40	High	n.s.
94	25	High	0.9
97	n.s.	30	1.2
100	n.s.	2.5	n.s.

Consider first the exposures performed at 2% chloride level. For the shorter exposure time a maximum in corrosion rate was observed around 91% to 94% RH and samples exposed at these RH values could not be evaluated at a longer exposure time due to cracking. The interpretation of the maximum is that below the maximum, the corrosion rate is under resistive control while above the maximum the high water content results in a limitation of oxygen transport. Worth noting is the unexpected high corrosion rate at 97% after 15 months of exposure. This can be explained by an also unexpected drop in capillary saturation from 1.0 at 3 month to 0.95 at 15 months.

For exposures performed at lower chloride levels, between 0.2% and 1.0%, a maximum corrosion rate is instead observed at 97% RH, a significantly higher humidity. Since according to these measurements a possible chloride threshold level definitely is below 2%, the results indicate that threshold levels should be evaluated at rather humid conditions (97%) despite the fact that the maximum corrosion rate at higher chloride levels is observed in the interval 91% to 94%.

Other studies have been performed to assess the corrosion rate of steel in concrete at different moisture levels ([4],[9–11]). Tuutti [4] added $CaCl_2$ to the mixing water of the mortar samples and exposed the samples to various moisture conditions. The steel bars were pickled before casting to remove the oxide scale. The corrosion rate was measured by repeated pickling and the maximum corrosion rates were measured at about 95% relative humidity. In higher and lower relative humidity, the corrosion rate was lower. The behavior that the corrosion rate reaches a maximum at a certain relative humidity and the corrosion rate is lower at other relative humidity is in agreement to the results here reported. The reported corrosion rates were about 40 µm/year for mortar samples with water cement ratio of 0.4 and Portland cement used as binder and about 30 µm/year for samples with water cement ratio of 0.7. Mortar samples made of 70% slag cement and 30% Portland cement had a corrosion rate of about 60 µm/year for samples with water cement ratio of 0.4 and about 40 µm/year with a water cement ratio of 0.7. The corrosion rates measured in this study for samples with 2 % Cl, 40 µm/year at 90% RH, are similar to the corrosion rate measured by Tuutti for samples with added $CaCl_2$ with the mixing water and exposed at 95% relative humidity.

Pettersson [9] used an electrochemical method, linear polarization resistance (LPR), to assess the corrosion of steel in mortar at different moisture levels. The mortar samples had Portland cement used as a binder and a water cement ratio of 0.5. The lowest chloride threshold level was measured to be 0.5 % Cl for samples exposed at 90% relative humidity. In higher and lower relative humidity, the chloride threshold level increased, this is also in agreement with the current results. It is worth mentioning that it may be difficult to measure a true corrosion rate with LPR since a constant beta value must be assumed. The beta value describes the relation between the corrosion rate and the polarization resistance that is dependent on the oxygen concentration. Therefore, the beta value must be measured for each moisture level in the used mortar to obtain a more reliable corrosion rate.

Consequently, this method is not particularly suitable for assessing the influence of relative humidity on the chloride threshold level.

Lopez [10] stated that pore saturation is influencing both the corrosion rate and the resistivity. Three pore saturation limits can be distinguished. A high pore saturation limit where the corrosion rate is high and a lower pore saturation where the corrosion rate is under resistance control. The third pore saturation limit where the corrosion rate is negligible. This is similar to the discussion of how the relative humidity is affecting the corrosion rate in the current study.

Nygaard [11] stated the temperature and the moisture condition in the concrete is not affecting the corrosion rate for passive steel. For actively corroding steel in concrete, the temperature and moisture condition is highly affecting the corrosion rate. This was also seen in the current study in terms of that the corrosion rate did not increase with higher moisture content for samples with no added chlorides.

The corrosion rates of samples with chlorides introduced by capillary suction and asymmetrical samples are shown in Table 5. The measured chloride concentration was 0.2% Cl for samples immersed in 0.08M Cl solution and 0.3% Cl for samples immersed in 0.12M Cl solution after vacuum treatment. There is no clear effect of the moisture condition on the corrosion rate. One reason can be that chlorides are unevenly distributed within the samples. The capillary saturation was generally lower compared to samples with mixed in chlorides and to samples with no added chlorides e.g. the capillary saturation for samples with 1.0% Cl was about 0.6 and for samples immersed in 0.08M Cl, the capillary saturation was about 0.4. The vacuum treatment may cause a coarsening of the pore structure [12] and thereby decrease the capillary saturation at a certain RH.

The corrosion rate of asymmetrical samples, where one side of the samples was covered with butyl tape, is also shown in Table 5. The anodic area should theoretically be at the covered site and the cathodic area at the uncovered surface. However, it was not possible to visually observe any difference in corrosion attack between covered and uncovered sides.

Table 5
Corrosion rate after approximately 15 months of exposure of samples with chlorides introduced by capillary suction and asymmetrical samples (n.s. = not significant).

RH	0.08M Cl µm/year	0.12M Cl µm/year	Asymmetrical, 0.2% Cl µm/year	Asymmetrical 0.6% Cl µm/year
75	n.s.	n.s.	-	-
85	2.0	n.s.	-	-
91	n.s.	2.2	n.s.	n.s.
94	0.7	n.s.	n.s.	0.7
97	n.s.	1.2	0.7	1.8
100	1.0	n.s.	-	-

3.4 Assessment of samples exposed in cyclic moisture condition

The corrosion rate of samples which were exposed to cyclic moisture conditions between 75% and 100% RH are shown in Table 6 together with calculated averages and maximum based on all RH exposures in the interval between 75% and 100% (Fig. 6) for comparison, at corresponding chloride levels. For all three chloride concentrations the corrosion rate was higher for cyclic conditions than for the average corrosion rate for samples with similar respective chloride concentration. The highest corrosion rate, 2.1 µm/year, were measured for samples with 0.6 % Cl which was considerably higher compared to the average corrosion rate for samples with 0.6 % Cl exposed in static moisture condition and even higher than the maximum value obtained at 97% RH, the most corrosive RH value. A possible explanation for this is that the optimum moisture condition where the corrosion rate is highest is obtained somewhere between 97% and 100% RH. This humidity range was not tested on samples in static moisture conditions but was likely obtained at certain time periods during cyclic exposure. Another explanation may be that an inhomogeneous electrochemical condition on the steel surface is obtained during cyclic wetting/drying periods due to an always ongoing transportation of water and ions. Subsequently, corrosion is more easily initiated. For comparison, Angst et al 2011 [13] monitored the corrosion potential of concrete samples exposed in cyclic moisture conditions. During the wet period samples were immersed in a chloride containing solution for 2 days followed by the dry period, 5 days in indoor air. The chloride concentration in the concrete was measured when the corrosion potential dropped in cathodic direction. Several types of concrete were tested; type most similar to the one used in the present study was a concrete made of Portland cement with a W/C ratio of 0.5. The measured chloride threshold level for this concrete ranged from about 1.5 to 2.5% Cl. This higher chloride threshold level compared to that here reported, 0.6% Cl, may be explained with the different experimental setups including difference in concrete cover thickness and frequency of the dry/wet cycle period. The chloride threshold levels reported by [13] for all types of concrete ranged from 0.8 to 3.6 % Cl by mass of binder.

Table 6
Comparison of corrosion rates obtained at cyclic exposure, alternating between 75% RH and 100% RH and corresponding stationary exposure in the interval between 75% RH and 100% RH.

Chloride concentration	0.2%	0.4%	0.6%
Cyclic exposure, µm/year	0.7	1.3	2.1
Average corrosion rate for samples exposed in all constant humidities µm/year.	0.4	0.7	0.4
Maximum corrosion rate in constant humidity, µm/year (at 97% RH).	1.0	1.2	1.6

4. Conclusions

Corrosion rate of steel in mortar was assessed by exposing samples consisting of cylindrical steel bars cast in mortar contaminated with chloride at different levels and exposed to atmospheres at different relative humidity (RH). The corrosion rate was calculated subtracting the effect of a preexisting oxide scale. The results permit the following conclusions.

Exposures in constant RHs from 75% to 100% show that the corrosion rate is moisture dependent with a maximum in the interval 91% to 97% depending on the chloride concentration. At higher chloride concentration (2%) the maximum is at the lower end of this RH interval while at lower chloride concentrations (0.1% to 1.0%) the maximum is at the higher end of this interval. The interpretation of the maximum corrosion rate is that below the respective relative humidity there is a resistive control while above the maximum the high water content results in a limitation of oxygen transport. This suggests that chloride threshold levels should be evaluated at rather humid conditions (97%) despite the fact that the maximum corrosion rate at higher chloride levels is observed in the interval 91% to 94%.

For cyclic moisture conditions between 75% and 100% RH the corrosion rate at 0.6% chloride was considerably higher than the maximum value obtained at 97% RH static conditions, the most corrosive RH value. This suggests that there is an overestimation of chloride threshold levels evaluated from exposures performed at stationary conditions.

Acknowledgements

This research was funded by Elforsk and SBUF, which is gratefully acknowledged by the authors. The authors would also like to acknoledge Mr. Bror Sederholm, Swerea KIMAB, for fruitful discussions and critical comments on the manuscript.

Highlights

- The corrosion rate of steel in mortar was measured by repeated pickling.
- The chloride threshold level should be measured in about 97% RH for static conditions.
- The corrosion rate was higher in dynamic moisture conditions compared to static.

References

[1] R.P. Bertolini, Luca. B Elsener, P Pedeferri, Corrosion of steel in concrete - Prevention, Diagnosis, Repair, first edit, Wiley-Vch, Weinheim, 2004.

[2] U. Angst, B. Elsener, C.K. Larsen, Ø. Vennesland, Critical chloride content in reinforced concrete — A review, Cem. Concr. Res. 39 (2009) 1122–1138. doi:10.1016/j.cemconres.2009.08.006.

[3] R.E. Melchers, C.Q. Li, Reinforcement corrosion initiation and activation times in concrete structures exposed to severe marine environments, Cem. Concr. Res. 39 (2009) 1068–1076. doi:10.1016/j.cemconres.2009.07.003.

[4] K. Tuutti, Corrosion of steel in concrete, Swedish cement and concrete research intitute, 1982.

[5] P. Marcus, Corrosion Mechanisms in Theory and Practice, third, CRC Press, Boca Raton, 2012.

[6] J. Ahlström, J. Tidblad, Galvanic corrosion properties of steel in water saturated concrete, Mater. Corros. (2013) 1–9. doi:10.1002/maco.201307141.

[7] G. Hedenblad, L.-O. Nilsson, DEGREE OF CAPILLARY SATURATION. Report TVBM-7005, 1985.

[8] T. Luping, L.-O. Nilsson, Chloride binding capacity and binding isotherms of OPC pastes and mortars, 23 (1993) 247–253.

[9] K. Pettersson, Service life of concrete structures in a chloride environment. Report 1:97, Stockholm, 1997.

[10] W. Lopez, J.A. Gonzalez, Influence of the degree of pore saturation on the resistivity of concrete and the corrosion rate of steel reinforcement, Cem. Concr. Reasearch. 23 (1993) 368–376.

[11] A. Michel, P. V Nygaard, M.R. Geiker, Experimental investigation on the short-term impact of temperature and moisture on reinforcement corrosion, Corros. Sci. 72 (2013) 26–34. doi:10.1016/j.corsci.2013.02.006.

[12] T.T. Basile, B.J. James, M. Jacques, A Coupled AC Impedance – Creep and Shrinkage Investigation of Hardened Cement Paste, Mater. Struct. (2003) 147–155.

[13] U.M. Angst, B. Elsener, C.K. Larsen, Ø. Vennesland, Chloride induced reinforcement corrosion : Electrochemical monitoring of initiation stage and chloride threshold values, Corros. Sci. 53 (2011) 1451–1464. doi:10.1016/j.corsci.2011.01.025.